



University of  
Stavanger

Faculty of Science and Technology

## MASTER'S THESIS

Study program/ Specialization:  
MSc Petroleum Engineering /  
Reservoir Engineering

Spring semester, 2015  
Open

Writer:

Javier Esteban Ramos

.....

(Writer's signature)

Faculty supervisor: Professor Svein M. Skjæveland

External supervisor(s): PhD. Alexey Khrulenko

Title of thesis:

**Reservoir Characterization and Conformance Control from Downhole Temperature Measurements**

Credits (ECTS): 30

Keywords:

Temperature, STARS, CMG, simulation,  
reservoir characterization, thermal, tracer,  
permeability, porosity, fracture, channel,  
modeling.

Pages: 63

+ enclosure: 0

Stavanger, June, 2015.

Date/year

Reservoir Characterization and Conformance Control from  
Downhole Temperature Measurements

By

Javier Esteban Ramos

Master Thesis

Presented to the Faculty of Science and Technology

University of Stavanger

University of Stavanger

June, 2015

## Acknowledgments

First of all, I thank God for helping me achieve all my goals. I would also like to thank Norway and the University of Stavanger for such a wonderful time, experience and learnings I take with me.

Many thanks to Alexey Khrulenko for welcoming me to realize this project under his supervision and for teaching me and helping me through the course of my research. Thanks also to Prof. Svein for being my faculty Supervisor and being always available when I needed him.

Thanks to my family for being so supportive and being my companion even when the distance separates us. Also thanks to Dannie for being my other half. And thanks to all my friends from Venezuela and my new friends from Norway for all the good times.

Thanks to all the Professors in the University of Stavanger who shared their wisdom with me during my master studies. Thanks to the International Office, the Department of Petroleum Engineering and the Student Office.

## Abstract

### **Reservoir Characterization and Conformance Control from Downhole Temperature Measurements**

Javier Esteban Ramos  
University of Stavanger

Faculty supervisor: Professor Svein M. Skjæveland  
External supervisor(s): PhD. Alexey Khrulenko

Temperature plays an important role in reservoir development since it affects fluid and formation properties and it is especially important for EOR deployment.

Downhole temperature measurements have been available for many years. However, there is still potential for better interpretation of temperature readings to obtain valuable information about the reservoir. This study aims to evaluate how temperature readings may be used as a source of valuable information for better reservoir characterization, taking advantage of accurate downhole temperature measurements in real-time mode.

The purpose of this work is to contribute to a better understanding of practical use of transient temperature measurements and how they may be used as a tracer to identify flow trends between producer-injector pairs.

In the present study the thermal simulator STARS (CMG) was used to study temperature transient effects in mechanistic non-isothermal models. Several scenarios of reservoir environment were evaluated: homogeneous, vertically heterogeneous, channel (high permeable layer connecting injector-producer well pair) and fracture (high permeable blocks of low pore volume connecting injector-producer well pair).

Those models had been waterflooded for about ten years and then the injection rate was increased for a short period of time while the temperature response was being sensed in the producer. This boost in injection rate is precisely done in order to evaluate how temperature pulse reaches the production well. Simultaneously with the injection boost an aqueous tracer's was injected for purposes of comparison between "temperature" and conventional tracers.

It was concluded that the fluctuations of cold water injection rate may generate temperature transient effects across the reservoir and, according to the reservoir properties (especially permeability and porosity), this drop may be observed in the producing well to identify certain types of reservoir heterogeneities such as a connecting fracture or high permeable channel. It was also observed that the temperature response time is faster in all cases compared to an aqueous tracer. Therefore, applying a cold water injection boost in a reservoir that has been waterflooded can be very useful for a further selection of an EOR treatment since this might help to identify fluid flow patterns more efficiently.

# Contents

Acknowledgments .....	I
Abstract .....	II
List of Figures.....	V
List of Tables.....	VII
Nomenclature.....	VIII
1. Introduction.....	1
2. Literature Review .....	2
2.1. Reservoir Temperature .....	2
2.2. Temperature Effects in the Reservoir .....	3
2.3. Enhanced Oil Recovery Methods Sensitive to the Temperature .....	4
2.4. Norwegian Continental Shelf Properties.....	6
2.5. Temperature Measurements and Interpretation .....	6
2.5.1. Temperature Sensors .....	6
2.5.2. Optical Fiber Measurement of Pressure and Temperature .....	7
2.5.3. Bottomhole Gauges.....	7
2.5.4. Metrology of Temperature Gauges.....	8
2.6. Thermal Properties of Rocks .....	8
2.6.1. Volumetric Heat Capacity.....	8
2.6.2. Thermal Conductivity .....	9
2.6.3. Thermal Diffusivity .....	10
2.6.4. Thermal Expansion Coefficient.....	10
2.7. Tracer Technology .....	10
2.7.1. Types of Tracers Available.....	12
2.7.2. Retention Caused by Partitioning Between Phases .....	14
2.7.3. Tracer Tests .....	15
2.8. Analytical Modeling for non-Isothermal Fluid Flow .....	15
3. Numerical Modeling.....	17
3.1. Reservoir Simulation .....	17
3.2. Reservoir Simulators .....	17
3.2.1. ECLIPSE Temperature Option .....	18
3.2.2. ECLIPSE Thermal Option .....	19
3.2.3. ECLIPSE's Thermal Properties and Features.....	19
3.2.4. STARS - Advanced Processes & Thermal Reservoir Simulator .....	20
3.2.5. GEM - Compositional & Unconventional Oil & Gas Reservoir Simulator .....	23

3.2.6.	Flexible Wellbore Model .....	24
4.	Methodology .....	27
4.1.	Reservoir and Fluids Properties Used to Develop the Models.....	27
4.2.	Models.....	30
4.2.1.	Homogeneous Model .....	30
4.2.2.	Heterogeneous Model.....	31
4.2.3.	Dykstra-Parsons Variation Models .....	32
4.2.4.	Channel Model .....	32
4.2.5.	Fracture Model.....	33
5.	Results and Analysis .....	34
5.1.	Influence of Heat Losses in Over-/Underburden and Heterogeneity .....	34
5.2.	Temperature Response of the Homogeneous Model.....	35
5.3.	Temperature Response of the Heterogeneous Model .....	37
5.4.	Temperature Response for the Dykstra-Parsons Variation Models.....	39
5.5.	Temperature Response of the Channel Model .....	40
5.6.	Temperature Response of the Fracture Models .....	44
6.	Conclusions.....	50
7.	Limitations and Future Works.....	51
	References.....	VIII

## List of Figures

Figure 1.	Plot of temperature gradients in a subsurface formation as a function of depth. Mean surface temperatures for various regions are provided in plot. ....	2
Figure 2.	Earth’s surface heat flow. ....	3
Figure 3.	Thermal properties of common materials.....	9
Figure 4.	Mass flow rate of water through a linear system.....	11
Figure 5.	Oil volumetric formation factor (a) and density (b) vs pressure. ....	28
Figure 6.	Oil viscosity vs pressure (a) and temperature (b).....	28
Figure 7.	Relative permeability curves for water (a) and liquid (b).....	29
Figure 8.	Homogeneous model showing permeability in x-direction. ....	31
Figure 9.	Heterogeneous model showing permeability in x-direction. ....	31
Figure 10.	Dykstra-Parsons models showing permeability in x-direction. ....	32
Figure 11.	Channel model showing permeability in x-direction.....	33
Figure 12.	Fracture model ( $\Phi$ 0.003) showing permeability in x-direction. ....	33
Figure 13.	Effects of heterogeneity and heat losses (over-, underburden) to resulting temperature distribution in cross-section between the producer-injector pair. ....	34
Figure 14.	Temperature sensing for the homogeneous model.....	35
Figure 15.	Temperature sensing during injection boost for the homogeneous model. ....	36
Figure 16.	Temperature readings in the wellbore (FLEXWELL) and reservoir (block temperature) at the end of the injection boost for the homogeneous model. ....	36
Figure 17.	Temperature sensing for the heterogeneous model. ....	37
Figure 18.	Temperature sensing for completion (2,6,2) during injection boost for the heterogeneous model.....	38
Figure 19.	Temperature readings in the wellbore (FLEXWELL) and reservoir (block temperature) at the end of the injection boost for the heterogeneous model.....	38
Figure 20.	Temperature distribution in cross-section between the producer-injector pair for Dykstra-Parsons variation models. ....	39
Figure 21.	Temperature sensing for the Dykstra-Parsons variation models. ....	40
Figure 22.	Temperature distribution for the channel model. ....	41
Figure 23.	Temperature sensing for the channel model. ....	41
Figure 24.	Temperature sensing for completion (2,6,2) during injection boost for the channel model. ....	42

Figure 25. Temperature sensing for completion {2,6,2} during temperature response time for the channel model. ....	42
Figure 26. Temperature response for layer 2. Showing temperature response after the injection boost period, time of response and maximum temperature drop due to the boost, for the channel model. ....	43
Figure 27. Tracer arrival time for the channel model.....	43
Figure 28. Temperature sensing for fracture model with different porosity.....	44
Figure 29. Temperature sensing for fracture model with porosity of 0.003.....	45
Figure 30. Temperature sensing for fracture cases with porosity of (a) 0.01, (b) 0.02, (c) 0.03 and (d) 0.05 within the fracture.....	46
Figure 31. Temperature sensing for fracture model with porosity of 0.1 within the fracture.....	46
Figure 32. Temperature sensing for permeability variations of (a) 250mD, (b) 500 mD and (c) 750mD in the 0.05 porosity fracture model.....	47
Figure 33. Tracer production rates for the fracture case with different porosity.....	48
Figure 34. Comparison between temperature and tracer arrival times for the fracture model with different porosity.....	49



# List of Tables

- Table 1. Capabilities of Sink/Source and Flexible Wellbore models. .... 25
- Table 2. Reservoir Properties Used in the Models ..... 27
- Table 3. Fluid Properties Used in the Models ..... 28
- Table 4. Well Definitions and Schemes Used in the Models ..... 29
- Table 5. Permeability for the Dykstra-Parsons Variation Models ..... 39

## Nomenclature

Specific notations are defined in the text; next to the equations. The following is a list of standard notations used in the document.

A	Area [m <sup>2</sup> ]
d	Diameter [m]
K	Permeability [m <sup>2</sup> ]
$K_{rel}$	Relative Permeability []
P	Pressure [Pa]
P <sub>c</sub>	Capillary Pressure [Pa]
q	Volumetric Flow Rate [m <sup>3</sup> /s]
r	Radius [m]
$R_s$	Solution Gas-Oil Ratio []
$R_v$	Volatilized Oil/Gas Ratio []
$S_{gcrit}$	Critical Gas Saturation []
$S_{lrg}$	total residual liquid saturation in the gas–oil system []
$S_{orw}$	residual oil saturation to water []
$S_w$	Water Saturation []
$S_{wcrit}$	Critical Water Saturation []
T	Temperature [°C]

### Greek Alphabet

$\rho$	Density [kg/m <sup>3</sup> ]
$\Phi$	Porosity []
$\mu$	Viscosity [cp]

## 1. Introduction

Temperature is an important parameter of the reservoir, as it can affect fluid (first of all, viscosity and phase behavior) and formation properties and therefore it affects production.

In the course of field development, reservoir temperature may significantly change due to injection of fluids for pressure maintenance. These changes may be quite significant and crucial for deployment of temperature-sensitive Enhanced Oil Recovery (*EOR*) methods such as: Low Salinity, Surfactant flooding, Polymer flooding or Gel treatment. In this case, non-isothermal reservoir models must be used to support the decision making prior EOR deployment.

On the other hand, temperature changes may serve as a source of valuable information about the reservoir. Recent developments in technologies for reservoir monitoring enable accurate downhole temperature measurements in real-time mode. At the present time, downhole temperature measurements are readily available for fields on the Norwegian Continental Shelf. However, there is a gap between the ability to measure temperature and the ability to convert this data into information about the reservoir that may be used for decision making.

The first part of the thesis is focused on literature review to address the following main questions:

- Why and when does reservoir temperature change?
- How to monitor and interpret temperature changes characterization?
- How are temperature changes accounted in reservoir simulation?

The second part of this work would be focused in modeling the behavior of temperature in a simulator software that allows to characterize reservoir properties such as channels, traps, etc. and later interpret how to use this information for implementing EOR processes in such reservoir.

Since evaluating the temperature is critical for EOR implementation and continuity, we can take advantage of the temperature measurements and use it, for example, as a tracer that allows us to study the developing of the processes and oil drive efficiency.

The purpose of this work is to contribute to a better understanding of practical use of transient temperature measurements which can be used as a tracer in the reservoir to identify flow trends between producer-injector pairs.

## 2. Literature Review

### 2.1. Reservoir Temperature

In a reservoir, it can be found different bodies with different thermal properties and behaviors (i.e. fluids, rocks). The reservoir is at a thermodynamic equilibrium prior to development, such temperature distribution within a reservoir varies with depth and is solely governed by earth heat flow and thermal conductivity. This temperature distribution can be estimated via the following equation:

$$T_{res} = T_s + (Thermal\ Gradient) * Depth \quad (1)$$

where,  $T_{res}$  is the reservoir's temperature in °F and  $T_s$  the surface's temperature in °F. Earth Heat Flow can be estimated with the equation

$$Earth\ Heat\ Flow = THC * (Thermal\ Gradient) \quad (2)$$

where, THC is the thermal heat conductivity.

Reservoir temperature can be obtained by direct measurements and is commonly found to increase by 0.6 to 1.6°F every 100 feet in many reservoirs. Figure 1 is a graphical representation of the increase in subsurface temperature with depth.

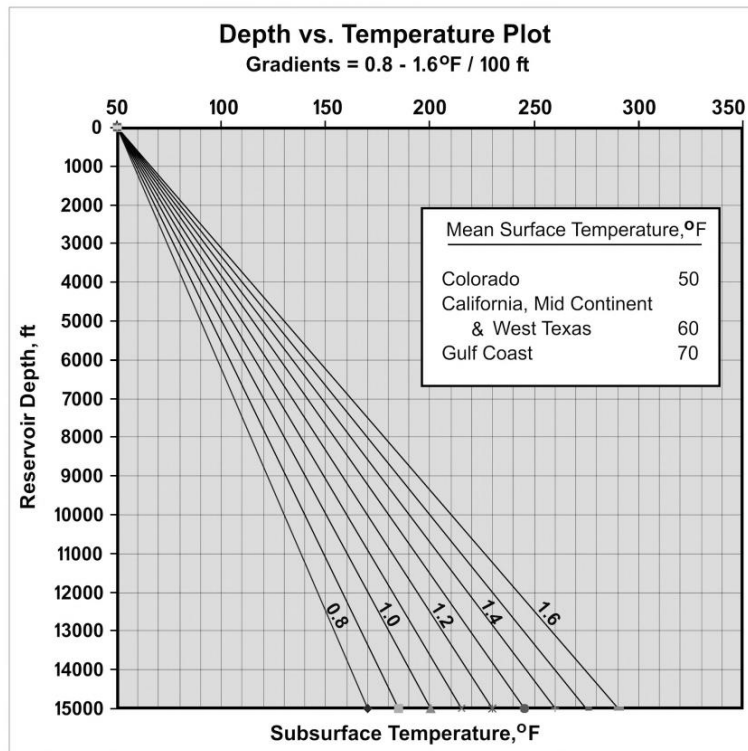


Figure 1. Plot of temperature gradients in a subsurface formation as a function of depth. Mean surface temperatures for various regions are provided in plot. <sup>[1]</sup>

Reservoir temperature refers to the temperature of the reservoir as a unit, since all bodies are usually in thermal equilibrium, however, it is a function of the depth, i.e. varies with the proximity to the core or geothermal activities. In a reservoir temperature is governed mainly by the proximity to earth's mantle, relative heat exchange capacities and thermal conductivities of the lithostatic sequence formations around the reservoir. In Figure 2 it can be seen how heat flows through earth's surface from earth's core.

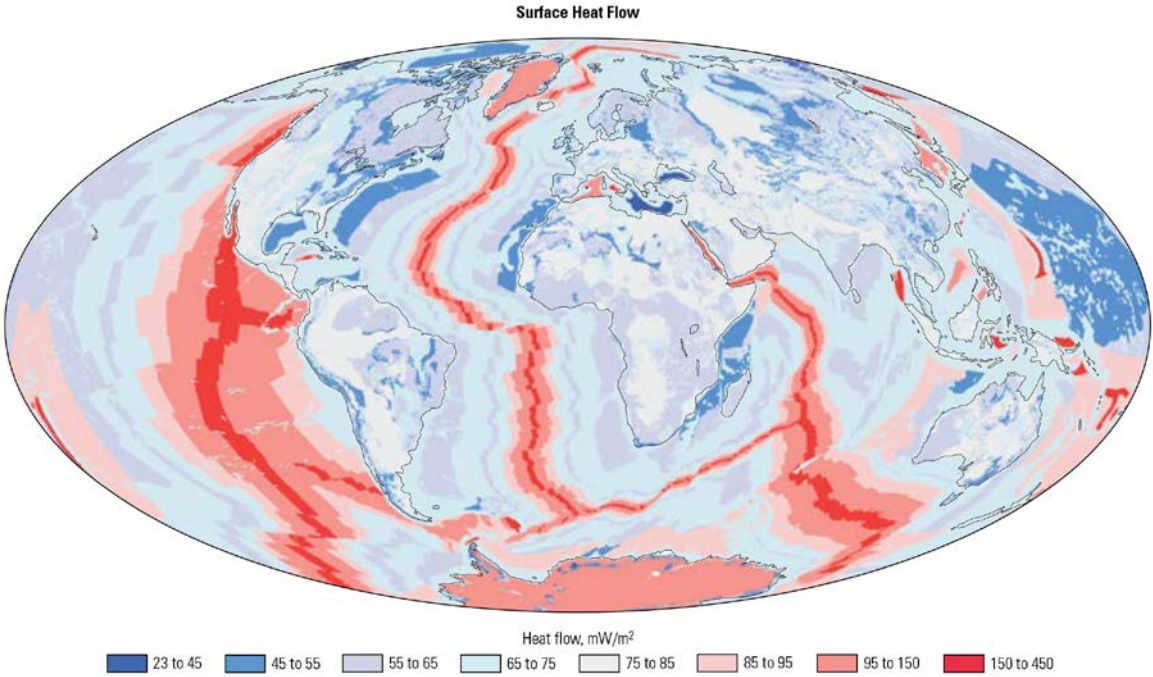


Figure 2. Earth's surface heat flow. [2]

Geothermal temperature is the measure of the temperature increase with depth as a result from heat being transferred from the Earth's core to the surface. To determine a precise geothermal gradient, the selected well must be shut in, without disturbance, for a period of time sufficient to let conduction effects equilibrate the temperatures.

### 2.2. Temperature Effects in the Reservoir

Temperature changes in the reservoir can affect fluids and rocks properties, for example, injecting water at a temperature considerably below the reservoir's temperature may change the behavior of the rocks and fluids in the reservoir; and this is why it must be accounted and analyzed in every stage of the reservoir production, especially when the implementation of EOR methods to produce the

reservoir is considered, since the analysis of the data may help to understand the flow between producer and injector well pair <sup>[3]</sup>.

Fluids are strongly affected by temperature through their viscosity, a measure of fluid's resistance to flow, which is a function of temperature. Fluid viscosity determines the mobility of a fluid in a porous media and is one of the major factors affecting reservoir production. A viscous crude would require more energy to flow than a lower viscosity oil therefore it is important to properly manage the temperature (as well as pressure) in a reservoir.

Also, heat exchange occurs in the boundaries of the reservoir, especially with the under- and overburden rocks which temperatures are different than those in the reservoir and also can exhibit different thermal properties.

Recently, interpretations of temperature in horizontal wells are reported to be useful to identify types of fluid flowing to a wellbore <sup>[3] [4] [5]</sup>. Hence, the need to correctly characterize this property and evaluate its effects on the production method.

### 2.3. Enhanced Oil Recovery Methods Sensitive to the Temperature

Temperature is critical for EOR implementation and continuity, since many of the fluid's properties are directly affected by temperature changes. Therefore, it is important to monitor or properly assess the temperature in the reservoir so it can be used as part of the screening criteria to select different EOR methods. Most relevant EOR methods sensitive to temperature are:

- Smart Water: Water with a special composition that includes Low Salinity Water Flooding (LSW), which implies injecting a lower salt content brine (with a lower ionic strength) which tends to favor recovery and High Salinity Water Flooding (HSW).
- Surfactant flooding, in which a small amount of surfactant is added to a brine to sweep the reservoir to reduce the interfacial tension between the oil and water and also alter the wettability of the reservoir rock.
- Polymer flooding, in which water viscosified with soluble polymers is used to increase its mobility with regards of the oil phase in place and maximize oil-recovery sweep efficiency.
- Gel treatment, used to treat matrix-rock problems or high permeability anomaly problems (fractures) by using gels to isolate parts of the reservoir.

- Foam, used to increase sweep efficiency of the injected gas, for blocking and diverting injected gas from entering high permeable zones or fractures, and in treating production wells suffering from unacceptably high gas oil ratio levels.

As commented before, temperature plays an important role in the implementation of such EOR methods.

- For LSW, most of the studies have been performed at temperatures below 100°C and it is believed that LSW at higher temperatures can result in no effects in the reservoir <sup>[6]</sup>. The reactivity of Ca<sup>2+</sup> increases with increasing temperature which results in less adsorption of polar components onto the clay <sup>[7]</sup>. For High Salinity Waterflooding, high temperatures contribute to the efficiency of the process <sup>[8]</sup>.
- For surfactant flooding, a surfactant or surfactant blend has to be tailored to the reservoir conditions (i.e. temperature, salinity and crude oil); and, when properly selected, it can handle high temperatures <sup>[9]</sup>. However, when not properly selected surfactant properties can vary unfavorably. Likewise, economics play a very important role when selecting the surfactant.
- For polymer flooding, there is an upper temperature limit (80 – 99°C) above which they are no longer chemically stable, this limit depends on the manufacturer and it must be determined if the polymer is thermally stable under reservoir conditions <sup>[10]</sup>.
- For gel treatment, the temperature dependency for most of the known gel systems follow an Arrhenius type equation ( $\exp(E_a/RT)$ ), where E<sub>a</sub> is the activation energy, T is the temperature and R is the gas constant. Reservoir temperature front is one of the critical factors for onset of gelation. Gelation time is highly influenced by temperature <sup>[11]</sup>.
- For foam, temperature is a critical parameter since it affects both the capacity to foam and the surfactant degeneration. The general trend is that the effect of foam decreases at increasing temperatures <sup>[12]</sup>.

Hence, to know the temperature behavior in the reservoir results crucial for the correct implementation of many EOR processes.

## 2.4. Norwegian Continental Shelf Properties

An extensive literature review about the Norwegian Continental Shelf (NCS) was made by Awan et al.<sup>[13]</sup> it can be summarized from it that most reservoirs in the NCS have the following properties:

- Light oil (32 to 41°API)
- Depths ranging from 1740 to 3800 m subsea.
- In terms of rock type classification, all the fields reviewed had high-permeability channels. Being Ekofisk a fractured reservoir with a low permeability matrix (0.1 md), while Gullfaks having the greatest range of permeability (80 to 4,500 md).

However, several reservoirs with depths beyond 4000 meters have been discovered, having Kristin 5000 m and reservoir temperature of 170°C. From the Norwegian Petroleum Directorate (NPD) it is assessed that on the NCS, in a normal trend, temperature increases by 25 degrees per kilometer of depth. Range of temperatures in most of the fields are between 70 to 170°C.

## 2.5. Temperature Measurements and Interpretation<sup>[14]</sup>

There are several tools and methods to measure temperature downhole, a short review on their performance is presented below:

### 2.5.1. Temperature Sensors

- Mechanical Transducers: The first bottomhole thermometers were mechanical. They were identical to bottomhole mechanical pressure gauges but with a thermometer instead.
- Thermistors: Temperature-sensitive resistive elements made of semiconductor material with a negative coefficient of resistance. They are based in the increased number of conducting electrons for a corresponding increase in temperature and operate up to 150°C.
- Resistance Temperature Detectors: These rely on the increase in resistance of metals in response to increasing temperature. They consist of a coil of fine metal wire or a film of pure metal deposited on a nonconductive surface. Usually encased in a probe directly exposed to the well fluids.



### 2.5.2. Optical Fiber Measurement of Pressure and Temperature

An optical fiber permanently deployed in the completion where sensors have no exposed electronic components making it more reliable. Furthermore, optical sensors are immune to shock, not prone to electromagnetic interference, and operable at high temperatures.

Fiber optic technology is based on exposing the fiber to periodic ultraviolet (*UV*) light patterns that induce a “grating” on it. Pressure and temperature variations change the reflection wavelength of the gratings and can be decoded with respect to the fixed, incipient operating wavelength. The system is self-referencing.

Every point distributed along the length of the fiber has the potential to generate a different temperature measurement. The advantages are measurement of a permanent temperature gradient over the length of the fiber and the ability to select specific measurement points.

### 2.5.3. Bottomhole Gauges

Pressure and temperature gauges can be linked to the downhole environment by several methods.

- Electric Line: Provides surface readout and can be conducted any time during the life of the well.
- Slickline: Performed with hanging gauges in situations that do not require surface readout. Slickline operations are more cost-effective than electric line's; however, the data quality usually does not match the readouts at surface, therefore, depth control is a critical factor.
- Coiled Tubing: As a popular alternative to drillpipe, coiled tubing is used to convey downhole gauges and other equipment in deviated holes when gravity is insufficient to pull the tools to the bottom of the well.
- Tractors: complements the use of coiled tubing in difficult, deviated completions. Tractors are self-powered and operated by electric line. They can negotiate bends, crawl up or down, and overcome the limitations of coiled tubing in long horizontal wells.
- Wireless Transmission: Attempts to avoid using an electric line. The downhole tool, a sub that is part of a Drillstem Testing (*DST*) string, features a pressure gauge, battery pack, telemetry, recorder board, and antenna. The antenna sends the signals collected from the pressure recorder at a frequency suitable for transmission through the formation strata. At the surface,

the signals are picked up by an array of suitably deployed stake antennae. Limited to land operations and depths of approximately 2,500 m.

- **Drillstem Testing:** A complex array of downhole hardware used for the temporary completion of a well. Provides a safe and efficient method to control flow while gathering essential reservoir data in the exploration, appraisal, and development phases of a reservoir or to perform preconditioning or treatment services before permanent well completion.

The temperature survey method most commonly used today in the industry is Distributed Temperature Sensors (*DTS*). *DTS* is a “technology for permanent monitoring that can provide temperature measurements over long intervals extending up to the complete length of the wellbore. Alternatively, an array of miniaturized digital temperature sensors can be used.”<sup>[15]</sup>

#### 2.5.4. Metrology of Temperature Gauges

By using sensors in immediate contact with the wellbore fluid, bottomhole-fluid temperature measurements are taken. These sensors have a minimum thermal inertia, of 1 or 2 seconds, to closely follow the variations of fluid temperature. Typical wellbore-fluid temperature measurements have a resolution in the range of 0.05°F and accuracy in the range of 1°F.

### 2.6. Thermal Properties of Rocks<sup>[2]</sup>

Rocks may exhibit macroscopic thermal anisotropy; i.e. different numerical values for thermal conductivity result from measurements across different pairs of opposing faces on a cube of the material and heat flows preferentially in certain directions through the rock. Such heterogeneity of rock thermal properties is closely related to variations in porosity<sup>[16]</sup>.

#### 2.6.1. Volumetric Heat Capacity

Volumetric Heat Capacity measures the amount of heat needed to raise the temperature of a unit volume (1m<sup>3</sup>) of a substance by 1°K. Basically, defines how a given volume of a substance stores internal energy while undergoing a given temperature change.

### 2.6.2. Thermal Conductivity

A quantitative connection between heat flow and temperature differences with units of W/m<sup>2</sup>K. It can be defined by considering a cube of homogeneous material with a temperature difference between two opposite faces  $\Delta T$ . The amount of heat flowing through the cube  $q$ , from the high- to low-temperature faces, is proportional to the temperature difference divided by the distance between the faces  $\Delta z$  [2]. Thermal conductivity of water is about 0.6 W/m<sup>2</sup>K. The thermal conductivity of rocks is generally higher (about 0.5 to 6.5 W/m<sup>2</sup>K). The equation for the thermal conductivity is

$$q = -k \frac{\Delta T}{\Delta z} \quad (3)$$

where the proportionality constant  $k$  is the block's thermal conductivity. Figure 3 shows the volumetric heat capacity and thermal conductivity for common materials.

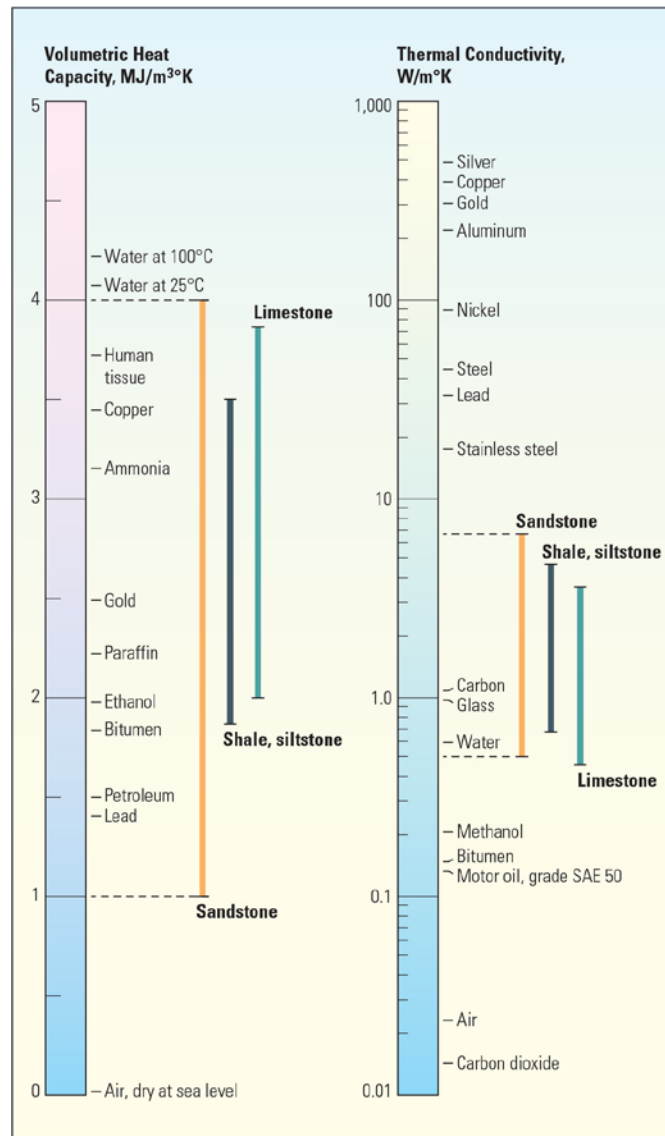


Figure 3. Thermal properties of common materials [2].

### 2.6.3. Thermal Diffusivity

Volumetric heat capacity and thermal conductivity combine to determine a third thermal property, called thermal diffusivity.

Thermal diffusivity is the ratio between thermal conductivity and volumetric heat capacity. It controls the rate at which temperature rises in a uniform block of material when more heat is flowing into the block than flowing out. It is defined by the expression

$$\alpha = \frac{k}{\rho c_p} \quad (4)$$

where  $k$  is thermal conductivity ( $\frac{W}{mK}$ ),  $\rho$  is density ( $\frac{kg}{m^3}$ ) and  $c_p$  is specific heat capacity ( $\frac{J}{kgK}$ ).

Together,  $\rho c_p$  can be considered the volumetric heat capacity ( $J/(m^3 \cdot K)$ )

### 2.6.4. Thermal Expansion Coefficient

Thermal expansion is the tendency of matter to change in volume in response to a change in temperature; through heat transfer <sup>[17]</sup>.

Thermal expansion coefficient measures a fractional change in linear dimension of a uniform cube for a unit temperature rise. Each side of the cube may expand by a different amount in anisotropic materials.

## 2.7. Tracer Technology <sup>[14], [18]</sup>

Tracer tests are used in determining the preferred flow paths between injectors and producers. It is done by adding a substance to the injected fluid that can be traceable once reached the producing well or wells to measure tracer effluent concentration profile. Tracer tests are used for the following purposes:

- to clarify connectivity between the wells
- to identify offending injectors (when a small transit time between a set of injector and producer occurred then it is highly probable there are fractures or a permeability trend); and
- to characterize the flood pattern and directional flow trends;

- to delineate the features of reservoir architecture (faults, fractures, permeability variations etc.) that may cause poor sweep efficiency;

There are different types of tracers that may be used in the reservoir. In this work, the temperature changes in the reservoir will be used as the tracer definition and it will be compared with an aqueous tracer.

Aqueous tracers are characterized generally because they do not react with other materials in the reservoir; they remain dissolved in the water and are immiscible with the oil. To model the behavior of the aqueous tracer, the Buckley and Leverett basic equation (1942) to describe the immiscible displacement in one direction for water displacing oil can be used. The equation determines the velocity of a plane of constant water saturation travelling through a linear system<sup>[19]</sup>.

The mass conservation of water flowing through volume element  $A dx$  (shown in figure 4), while gravity effects are neglected, water and oil are immiscible and incompressible and temperature is constant, can be expressed as:

$$\text{Mass flow rate In} - \text{Out} = \text{Rate of increase of mass in the volume element} \quad (5)$$

Which can be formulated as

$$\frac{dq}{dx} = A\phi \frac{dS_w}{dt} \quad (6)$$

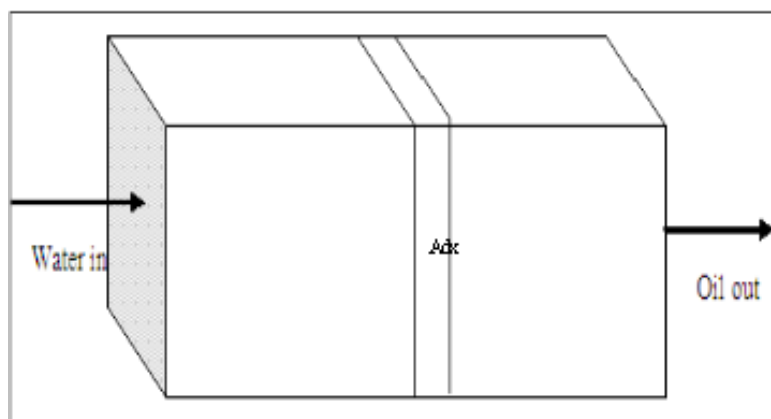


Figure 4. Mass flow rate of water through a linear system.

When the equation is rewritten by introducing the water fraction flow, the following Buckley-Leverett equation can be obtained, which implies that the velocity of a plane of constant water saturation is directionally proportional to the derivative of the fractional flow evaluated for that saturation under a constant rate of water injection<sup>[18]</sup>.

$$\frac{dx}{dt} = \frac{q}{A} \phi \frac{df_w}{dS_w} \quad (7)$$

When an ideal tracer is added to the injected water, the equation for the tracers is expressed as:

$$\frac{d}{dt} [\phi S_w C + (1 - \phi)C] + \frac{q}{A} \frac{df_w}{dx} C = 0 \quad (8)$$

where C is the Tracer Concentration.

If it is assumed that the tracer concentration does not affect the water flow rate, it is not soluble in water phase and the tracer does not absorb subsurface solids, the equation can be simplified as:

$$\frac{\partial C}{\partial t} + \frac{q}{A} \frac{f_w}{\phi S_w} \cdot \frac{\partial C}{\partial x} = 0 \quad (9)$$

It can be found that the injecting water will move with a velocity equals to  $qdf_w/A\phi S_w$  and the aqueous tracer will move with velocity of  $qf_w/A\phi S_w$ , which means that the velocity of water is proportional to  $df_w/dS_w$  while the velocity of the tracer is proportional to  $f_w/S_w$ .

Lack of adequate information on fluid flow is a general problem for reservoir engineers. Information obtained from tracer test is unique, and relatively cheap when it comes to reduce uncertainty in the reservoir.

### 2.7.1. Types of Tracers Available

Tracers may be classified as passive or active. A passive tracer follows the fluid phase in which it is injected without react with fluids or rocks in the reservoir while active tracers interact with the other fluids in the system or with the rock surface. A passive tracer must have a very low detention limit, must be stable under reservoir conditions, must follow the phase that is being tagged and have a minimal partitioning into other phases, must have no adsorption to rock material, and must have minimal environmental consequences.

#### 2.7.1.1. *Radioactive Water Tracers.*

Radioactive tracers tends to behave nearly as passive tracers (follows water it is going to trace). Very few compounds will behave as passive tracers in all situations, but near-passive tracers will, in many applications, work satisfactorily. If the objective is to measure fluid communication exclusively, a near-passive tracer may be as good as a true passive tracer. The compound that best fulfills the passive tracer requirements is tritiated water (*HTO*). The passive water tracer mimics all movements and interactions that the water molecules do in the traced water volume.

#### 2.7.1.2. *Chemical Water Tracers.*

A chemical identifiable markers may be added to injected water to trace water flow. The most applied nonradioactive anion is the thiocyanate anion. It has a low natural background in the reservoir, and a detection limit in the range of 1 µg/L (1 ppb) can be obtained by electrochemical detection after separation on a high-pressure liquid chromatograph. In the reservoir.

#### 2.7.1.3. *Radioactive Gas Tracers.*

Several authors report the use of radioactive gas tracers in oilfield applications. The tracers most frequently applied have been tritiated methane, tritiated ethane, and 85Kr. The tritium-labeled compounds may be measured directly in the gas phase by proportional counter techniques. To obtain the low detection limit normally required in well-to-well tracer studies.

Other alternatives are the noble gases. The noble gases are virtually inert against chemical reaction. 85Kr has a half-life of 10.76 years and is a beta emitter with an energy of 687 keV. The two xenon isotopes, 127Xe and 133Xe, are also inert noble gases that may be applied in special situations in which rapid response is expected.

#### 2.7.1.4. *Chemical Gas Tracers*

As early as 1946, Frost reported the use of helium as a tracer under gas injection. The background of the noble gases in the reservoir is, however, generally too high, which makes nonradioactive noble gases unattractive as tracers. These gases can be applied only when the dilution volume is very small.

One group of tracers that has found wide application and has become the most widely applied of the chemical gas tracers today is the perfluorocarbon (*PFC*) group of molecules. *PFCs* have excellent tracer properties such as high stability, chemical inertness, and high detectability. *PFCs* are liquids with a density of approximately 1.8 g/mL at standard conditions; therefore, they can be injected into the reservoir with high-pressure liquid pumps.

### 2.7.2. Retention Caused by Partitioning Between Phases

When tracers are flowing in the reservoirs, it is normally a requirement that the compounds follow the phase they are going to trace. The best example of a passive water tracer is *HTO*. The *HTO* will, in all practical aspects, follow the water phase.

For gas tracers, there are not known passive tracers. All gas compounds will, to a certain degree, partition between the phases. The most ideal gas tracer is tritiated methane. This gas tracer follows the methane component in the gas phase closely, and the *PVT* properties of this gas tracer can be found with ordinary *PVT* calculations.

Water tracers, like gas tracers, may partition to the oil phase. Many water tracers exist that behave almost as ideal tracers. Retention factors,  $\beta$ , may be derived from equation 10 on the basis of production profiles.

$$1 + \beta = \frac{V_T}{V_S} \quad (10)$$

Here,  $V_T$  is the retention volume for the tracer candidate and  $V_S$  is the retention volume for the standard reference tracer. The retention volume for the standard reference tracer (nonpartitioning) may further be regarded as the volume of the mobile phase,  $V_M$ , in this system. If other retention effects can be excluded, the retention factor is an expression for the delay caused by partitioning the tracer between the mobile and the stationary phase. <sup>[14]</sup>

We can also use temperature as a tracer to identify reservoir heterogeneities since the temperature front will eventually reduce the reservoir temperature at the producing well; when injecting cold water into a hot reservoir.



### 2.7.3. Tracer Tests

The test consist in adding to the injection fluid one or several elements easy to detect, in known concentrations. Such fluids would be later recovered by the producing well, where some specific instruments will detect them. The movement of the tracer reflects the movement of the injected fluid; so this test is an efficient way to monitor and define the dynamic behavior of the fluids in the reservoir and determine the main flow parameters that impacts the injection process.

Using temperature as a tracer, the process would be similar, injecting a colder fluid to the reservoir will generate a variation in temperature that will eventually reach the producer well, which should be equipped with a Drillstem Testing along the perforations so it can determine when and where the temperature drop occurs first.

## 2.8. Analytical Modeling for non-Isothermal Fluid Flow

Lauwerier<sup>[20]</sup> published one of the first solutions to the temperature profile for the injection of hot water into an oil bearing layer. He used the conductive form of heat loss in a linear flow geometry assuming an infinite thermal conductivity in the vertical direction within the permeable sand. No horizontal conduction in the direction of the flow was considered.

Rubinstein<sup>[21]</sup> formulated the Lauwerier model for the radial flow case, assuming constant isothermal conductivities in the reservoir and surrounding strata. His solution is in terms of heating efficiency only.

Horizontal conduction was taken into account analytically by Zolotukhin et al<sup>[22]</sup>, who obtained an expression in cylindrical coordinates using an overall time dependent heat transfer coefficient. Their description of the temperature profile is expressed in an integral form and does not lend itself to easy evaluation. In most solutions the horizontal conduction is neglected or the solution allows for one injection temperature only. As it is well known it can take several days before a constant injection temperature reach the perforations.

Platenkamp<sup>[23]</sup>, describes later on an expression for cold water injection entering a hot reservoir, where three heat exchange processes exist (thermal conduction, convective heat transfer between fluid and solid matrix and heat transfer caused by friction) for single- and multi- layered reservoirs.

He showed that, since convection is the dominant mechanism, an estimate of the position of the temperature front ( $X_f$ ) can be made using a simple heat balance as:

$$X_f = \sqrt{\frac{\rho_w C_w}{\rho_e C_e}} \emptyset R_{inj} \quad \text{for the radial model; and} \quad (11)$$

$$X_f = \frac{\rho_w C_w}{\rho_e C_e} \emptyset D_{inj} \quad \text{for the Linear model.} \quad (12)$$

Here  $\rho_w$  is the specific heat of water,  $C_w$  the density of water and the product  $\rho_e C_e$  is the effective heat capacity of the matrix rock filled with water.  $R_{inj}$  and  $D_{inj}$  denote the distance of the flood front from the water injector.

The evaluation of the equations of those works is beyond the scope of this work, here, it would be tried to evaluate the usability of the temperature drop in the reservoir to characterize the heterogeneities that can be present in the reservoir.

Arihara<sup>[24]</sup> experimentally proved that the core is cooled down more efficiently when the injection rate is lower. When water is injected with a constant mass rate, the lower the injection temperature is than the surroundings temperature, the more efficiently heat is extracted from the surroundings within a certain period of time.

## 3. Numerical Modeling

### 3.1. Reservoir Simulation

One task for Reservoir Engineering is to evaluate the behavior of the reservoirs under different production schemes. Today, in order to better understand that, there exist several programs that allow to better understand and model such behaviors; called Reservoir Simulators.

Reservoir simulation is based in the construction and run of a model with similar characteristics to the one we want to produce so it can be obtained representative and useful results to further develop the field efficiently. The mathematical model used in a simulator is a group of differential equations, which under certain initial and boundary conditions, describe the basic physical principles in a reservoir; such as energy and momentum conservation and state equations.

### 3.2. Reservoir Simulators

Currently, there are many software solutions capable of modeling reservoir performances. These can be divided, basically, into three groups:

- Black oil
- Compositional
- Thermal and enhanced recovery.

The two major simulator software suites used nowadays belong to Schlumberger (*SLB*) and Computer Modeling Group (*CMG*). Being Eclipse E100, E300 and E500 *SLB*'s flagships and IMEX, STARS and GEM *CMG*'s.

Both ECLIPSE and STARS work under the same energy equations balance principle. The equations used to describe thermal processes are similar to the compositional but there are three important differences: the addition of an energy variable and an energy equation; the presence of a water component in the gas phase as well as the water phase; and temperature dependence of properties. The variables to compute are: Pressure "*P*", molar densities "*m1...mN*", water molar density "*mw*" and the density of rock's inner energy "*e*". For each block there will be  $N+3$  variables, to get those variables

it is needed to solve, iteratively, N+3 nonlinear conservation equations. Also, the simulator calculates and updates oil and gas viscosities.

### 3.2.1. ECLIPSE Temperature Option

The Temperature option enables ECLIPSE to model temperature effects. The major effect of temperature changes in the vicinity of the injection wells is to modify the fluid viscosities. In addition, changes in the reservoir temperature will induce additional stresses within the reservoir which may modify the rock properties. Both the oil and water viscosities can optionally be specified as functions of temperature. The Temperature option is handled differently in the two simulators:

- In ECLIPSE 100 an energy conservation equation is solved at the end of each converged timestep, and the grid block temperatures are updated. The new temperatures are then used to calculate the oil and water viscosities for the subsequent timestep.
- In ECLIPSE 300 the energy conservation equation is solved simultaneously with the flow equations.

In both cases, the rock and all fluids in a grid block are assumed to be at the same temperature. Water is allowed in the vapor phase, the equilibrium state depends on the temperature, the reservoir temperature changes if the reservoir pressure changes. Similarly the injection temperature changes as the well BHP changes. A thermal flash is performed to determine the equilibrium state. K-values are calculated from  $R_s$  and  $R_v$  values as functions of pressure and temperature.

In this option, Thermal Conduction is optional (since heat in the rock is often a small effect compared with the convection of heat with the injected water) and to activate it, it must be specified the cell rock and fluid thermal conductivity in the GRID section. Also, Heat losses to and from areas outside the reservoir model are not taken into account and, if needed, can be modelled by extending the model so large blocks can act as a heat sink. These additional blocks have to be active cells (pore volume > zero), but the permeability may be set to zero. And, the initial temperature is either assumed to be constant throughout the reservoir or can be specified as function of depth. The temperature of the injected fluid can be specified for each well.

### 3.2.2. ECLIPSE Thermal Option

This option is used to simulate Thermal Recovery Processes in heavy oil reservoirs, where the oil viscosity is high at reservoir temperatures, but reduces as the temperature increases. Among the processes it can be found: steam injection, steam flood, steam assisted gravity drainage (SAGD), hot fluid or gas injection, well bore heaters, combustion, foamy oil, dual porosity grids, etc.

The thermal simulator does not use an equation of state to determine the thermodynamic properties. K-values must be supplied to determine equilibrium and densities, viscosities and enthalpies for each component in each phase.

The phase properties used in the residual and jacobian equations (that is the fluid volume and the flow terms) can be calculated from the component properties once the mole fractions of each component in each phase have been determined.

The rate of flow of a component into a production well from cell is obtained by summing the component flow over all phases. The heat conduction term for each cell is given by summing conduction between all neighboring cells.

### 3.2.3. ECLIPSE's Thermal Properties and Features

Rock heat capacity is defined when the enthalpy per unit volume of rock equation is solved after the volumetric heat capacity, the temperature coefficient and the reference temperature are specified.

Cell average thermal conductivity is defined, which is used to determine the thermal transmissibilities. Depending on the option activated, thermal transmissibilities can be multiplied by a saturation-dependent factor.

Heat loss to the overburden, underburden and sides of the reservoir can be modeled. Number of rock types outside the reservoir can be defined. Each rock type can have different properties. Which cells on the edge of the reservoir connect to each rock type can be defined, and the local grid refinement connection data for these cap and base rocks can also be specified. Two methods can be used to calculate the heat loss, a numerical method and an analytic method.

### 3.2.4. STARS - Advanced Processes & Thermal Reservoir Simulator <sup>[25]</sup>

STARS is used for thermal and advanced process simulations. STARS is a thermal, k-value (*KV*) compositional, chemical reaction and geomechanics reservoir simulator. Designed for modelling of recovery processes involving the injection of steam, solvents, air and chemicals. The robust reaction kinetics and geomechanics capabilities make it a complete and flexible reservoir simulator.

Unlike ECLIPSE, STAR does not need a thermal option to be activated since it was designed to simulate processes such as: Steam Assisted Gravity Drainage (*SAGD*), Expanding-Solvent *SAGD* (*ES-SAGD*), steam, hot water, & hot solvent injection, cyclic Steam Stimulation (*CSS*), thermal VAPEX, in-Situ combustion (air injection), High & Low Temperature Oxidation (*HTO* & *LTO*), among others.

*STARS* have a solid rock-fluid interaction for temperature and/or composition dependent relative permeability, advanced  $K_{rel}$  and  $P_c$  hysteresis options for wetting and non-wetting phases, modelling of countercurrent flow, temperature and viscosity dependence for molecular diffusion, oil, water and mixed wettability options, etc.

Rock heat capacity is optional and can be specified by coefficients in the correlation for volumetric heat capacity of solid formation (rock) in the reservoir. Heat capacity of shale when a net-to-gross option is used.

Thermal conductivities of rock, solid and fluid phases are optional. It can be specified the rule used to mix thermal conductivities of rock and phases, the choice of mixing rule affects somewhat the meaning of the individual rock/phase thermal conductivity values or it can be set a simple volume-weighted mixing rule for thermal conductivity.

Overburden heat loss is optional, heat loss directions and over/underburden thermal properties for the semi-analytical infinite-overburden heat loss model can be defined and the overburden temperature and critical temperature difference can be controlled. Heat loss properties to the outer grid block faces at the reservoir top and bottom can be defined as well as in any indicated direction.

Volumetric heat capacity of formation adjacent to the reservoir in the indicated direction is also applicable. The lower limit is 0 (no heat loss), and the suggested upper limit is  $108 \text{ J/m}^3\text{-}^\circ\text{C}$ . For heat loss calculations, initial temperature of formation adjacent to the reservoir is needed.

Several thermal properties can be included in the simulation, among the most important we found the following.

#### 3.2.4.1. *Relative Permeability Temperature Dependence*

Specify the temperature dependence for critical saturations and endpoints. For the size of the mobile regions  $1-S_{wcrit}-S_{orw}$  and  $1-S_{gcrit}-S_{lrg}$ .

#### 3.2.4.2. *Temperature and Viscosity Dependence of Diffusion*

It can be specified temperature and viscosity dependence of molecular diffusion for any component in the fluid phase and phase. Or temperature dependence can be applied to molecular diffusion by multiplying by ratio  $(T/T_{refabs})$ , where  $T$  is the current temperature and  $T_{refabs}$  is the reference temperature  $T_{ref}$  converted to absolute degrees.

Viscosity dependence is applied to molecular diffusion by multiplying by ratio  $(\mu_{ref}/\mu)$ , where  $\mu$  is the current phase viscosity and  $\mu_{ref}$  is the reference phase viscosity (cp).

#### 3.2.4.3. *Temperature-dependent Properties*

Temperature dependence of geomechanical properties can also be specified i.e. which geomechanical properties will vary with temperature.

#### 3.2.4.4. *Thermal Expansion Coefficient*

When the temperature changes, the deformation as well as stress of rock also changes. Such changes strongly depend on the thermal expansion coefficient of a rock type. Thermal expansion coefficient can be specified for a rock type due to the thermal effect. The Coefficient value must be entered when the thermal effect is taken into account in the geomechanical model. When the keyword is absent, changes in thermal do not affect to the rock at all.

#### 3.2.4.5. *Temperature of Injected Fluid (Optional)*

To specify the temperature of injected fluid in the wells is optional. The wells must be injectors. A well must have been fully specified before its injection temperature may be modified.

#### 3.2.4.6. *Viscosity*

Water phase viscosity tends to be relatively constant at 1 cp, and decreases as far as 0.1 cp at 300°C. The main purpose of allowing entry of water viscosity data is to account for the various brine concentrations encountered in different reservoirs.

The STARS model has the following data entry options:

- Use internal table of  $\mu_w$  versus  $T$ , with a possible dependence on salt concentration which can be significant.
- Use the correlation  $\mu_w = a \cdot \exp(b/T)$ , where  $T$  is in absolute degrees.
- Enter directly a table of  $\mu_w$  versus  $T$ .

Gas phase viscosities usually are much smaller than liquid phase values, and hence will tend to dominate the flow if gas phase is mobile. As a consequence, pressure gradients may be high when gas is immobile, but will certainly be low when gas is flowing. Gas phase viscosities have values around 0.01 cp.

#### 3.2.4.7. *Thermal Conductivity*

Thermal conductivity determines the flow term  $K\Delta T$  due to diffusion of energy from a region of high temperature to low temperature. The only other way for energy to flow in situ is by convection. In field-scale steam problems convection usually dominates conduction, at least in the direction of flow. In field-scale combustion, the temperature profile at the fire front can be determined largely by conduction, but this temperature profile is almost never resolved because the grid blocks used are too large. For these reasons, conduction is rarely a major mechanism in field-scale problems. Conduction can play a significant role in both steam and combustion at the laboratory scale, since the length scale is much smaller than in the field.

There are two options for calculating an overall thermal conductivity from phase values, Linear and non-linear. Basically the linear option assumes that all phases (including solid) are randomly mixed in a porous medium while the nonlinear option implies some type of correlated distribution of phases (reflecting the fact that the liquids tend to wet the rock).



#### 3.2.4.8. Overburden Heat Loss

A semi-analytical model is used for heat transfer to or from an adjacent formation of infinite extent. It assumes a temperature profile in the base or cap rock as a function of time and distance  $z$  from the reservoir interface.

#### 3.2.5. GEM - Compositional & Unconventional Oil & Gas Reservoir Simulator <sup>[26]</sup>

GEM is a reservoir simulation software for compositional and unconventional modelling. GEM is an advanced general Equation-of-State (*EoS*) compositional simulator that models the flow of three-phase, multi-component fluids. GEM can model any type of recovery process where effective fluid composition is important.

GEM simulates structurally complex and varying fluid combinations including processes in which the effects of inter-phase mass transfer (i.e. changing fluid phase composition) are important. GEM can model laboratory scale projects, pilot areas, elements of symmetry, or full-scale field studies, replicates reservoir physics and chemistry to assist in optimizing field, surface operating conditions and overall recovery, improves understanding of fluid property composition and behavior, simulates complex reservoirs to identify optimal reservoir processes, models naturally and hydraulically fractured reservoirs, increases estimated NPV through accurate phase behavior models and optimizes field and surface operating conditions for improved overall recovery.

It can be applied in simulation of unconventional reservoirs (Shale oil, gas & shale liquids, Liquids rich, Tight oil a gas, Naturally & hydraulically fractured reservoirs, Coal Bed Methane) and in dry gas, gas condensate & volatile oil (Gas cycling and re-cycling, condensate blocking, underground gas storage, fractured gas condensate wells and gas-oil gravity drainage).

In GEM, the following temperature properties can be defined:

- Thermal rock properties such as heat capacity and thermal conductivity of rock and fluids.
- Heat loss to the surrounding rocks (from all fundamental grid edge blocks, bottom and top of the reservoir).
- Thermal expansion coefficient of the formation, pressure-temperature cross-term coefficient of the formation effective porosity and reference temperature used in calculation of thermal expansion by geomechanics module.

- Heating values (heat of combustion) for each component to calculate the separator gas stream heating value by simple mole fraction averaging.
- Reservoir temperatures and depths at which temperature is known.
- Initial reservoir temperature at any block.
- Critical temperature multiplier, used with the single phase identification method and with single hydrocarbon phase relative permeability interpolation. This allows input of a factor which multiplies this calculated critical temperature to modify the point at which a single hydrocarbon phase is identified as an oil or a gas.
- Temperature dependence for geomechanical properties.
- Thermal expansion coefficient for a rock type due to temperature changes.
- Bottomhole temperature of the injected fluid into the wells.

Thermal option can be turned on and there must be specified the coefficients for ideal enthalpy calculations. This option is used to calculate temperature distribution in the reservoir for the compositional processes where reservoir temperature could change with time. The equations to be solved are: volume constraint equation; the volume of fluids must equal the pore volume, component flow equations; material balance equations for oil, gas and water components, energy balance equation including convection, conduction and heat losses and phase equilibrium equations.

### 3.2.6. Flexible Wellbore Model <sup>[27]</sup>

The wellbore model used in STARS under the name of FLEXWELL, encompasses a model that is solved independently but is fully coupled with a thermal reservoir simulator. The wellbore can contain up to three tubing strings in an annular space that runs in any direction (vertical, horizontal, slanted, undulating) locally, with possible laterals, and each flowing stream may be an injector or a producer operated at various conditions.

There are no restrictions on tubing lengths or how the wellbore intersects the reservoir grid. The tubing strings may have various lengths, may be fully or partially insulated and may have varying diameter along the length. The annulus may have casing, cement and varying diameter along the length. Radial heat flow is affected by wall thickness, insulation and cement.

The flow regime is a function of liquid and gas velocities for each flowing stream and is used to calculate frictional pressure drop as well as axial and radial heat transfer. The model also handles transient wellbore behavior which may be significant for cyclic processes.

Annulus and tubing string are divided into sections according to perforations specified in the data. Equations corresponding to all streams and sections of each FW are solved simultaneously; each FW equation set is solved separately from each other and independently from the reservoir. Spatially, all Flexible Wellbores are fully coupled to the reservoir through an annulus-reservoir flow term.

Annulus-reservoir communication is along the full wellbore length. Whether the exchange is both fluid and heat depends on the data input. When a perforation is specified as closed then only conductive heat is transferred; when a perforation is open then fluid and its convective heat can flow.

During solution of the Flexible Wellbore equations there is enough information about the wellbore conditions that cross flow, phase segregation and transient behavior can be handled correctly. In some processes or wellbore configurations these mechanisms are quite important to both the well and reservoir solution.

### 3.2.6.1. Application

Flexible Wellbore should be used when the wellbore flow is more complex and significantly impacts the reservoir behavior. Table 1 compares capabilities of the Sink/Source well and Flexible Wellbore models:

Table 1. Capabilities of sink/source and flexible wellbore models.

	Sink/Source well	FLEXWELL
Gravity	Explicit head	Implicit
Friction-heatloss	Optional	Automatic
Cross flow Wellbore-Reservoir	Optional (simple)	Automatic
Trajectory	Optional	Optional
Multilaterals	Optional	Optional
Transients	Not possible	Automatic
Fluid Segregation	Not possible	Automatic
Tubing	Not possible	Maximum 3
Wellbore heatloss and friction, wellhead to pay top	Optional	Optional
Orifice flow Annulus-Reservoir	Optional	Optional
Orifice flow Tubing-Annulus	Not possible	Optional
Well plugging by solids	Not possible	Optional

The Flexible Wellbore model will be most useful for processes that need tubing(s), fluid segregation, correct cross-flow handling, well plugging and transient behavior.

### 3.2.6.2. Numerical Behavior

Depending on the data used, numerical performance of the Flexible Wellbore versus the Sink/Source well model can vary, because of the degree of complexity solved by each model. When more complex data which encompasses cross-flow and phase segregation in the wellbore (undulating well), the conventional Sink/Source well model does not handle it correctly since its numerical difficulty. The numerics become even more difficult when different perforations cross-flow at different times <sup>[28]</sup>. The Sink/Source case used a conventional wellbore model without any special options such as friction pressure drop, heatloss and cross-flow calculations. On the other hand, the Flexible Wellbore model takes care of these mechanisms automatically. This different wellbore treatment might account for the temperature differences. Hence, the Flexible wellbore model can handle data complexity more accurately in such cases.

## 4. Methodology

During the realization of this project, several properties and arrangements were used in order to determine the most suitable case to start the simulation cases. It is of IRIS knowledge, among other companies and experts, that in order to get characteristic results it is sometimes better to use simple models that can accurately simulate the process; avoiding long run times and CPU usage.

### 4.1. Reservoir and Fluids Properties Used to Develop the Models

The pattern selected consists of a lineal arrangement with two vertical wells, one injector and one producer, in a matrix of 15 in x-direction, 10 in y-direction and 5 in z-direction. Common properties used for rock and fluids are listed in tables 2 & 3.

*Table 2. Reservoir properties used in the models.*

Block widths	
I	28 m
J	28 m
K	15 m
Top	2900 m
Formation Compressibility	$21.750 \times 10^{-6} \text{ kPa}^{-1}$
Porosity Range	25 to 48 %
Pressure at 2900 m	28420 kPa
Permeability	Varying for different cases
Reservoir Temperature	114°C
Average Pressure	28520 kPa
Water/gas cap	Not present
Volumetric Heat Capacity	$1.000 \times 10^6 \text{ J}/(\text{m}^3 \text{ }^\circ\text{C})$
Thermal Conductivity	$3.456 \times 10^5 \text{ J}/(\text{m day } ^\circ\text{C})$
Underburden Heat Loss	$2.900 \times 10^6 \text{ J}/(\text{m}^3 \text{ }^\circ\text{C})$
Underburden Thermal Conductivity	$8.840 \times 10^4 \text{ J}/(\text{m day } ^\circ\text{C})$
Overburden Heat Loss	$2.800 \times 10^6 \text{ J}/(\text{m}^3 \text{ }^\circ\text{C})$
Overburden Thermal Conductivity	$8.640 \times 10^4 \text{ J}/(\text{m day } ^\circ\text{C})$

Table 3. Fluid properties used in the models.

	Oil	Water	Tracer	Gas
API (°API)	28	-	-	-
Molecular Weight (kg/gmole)	0.21956	0.018	0.018	0.02028
Critical Pressure (kPa)	0	22063.2	22063.2	4543.26
Critical Temperature (°C)	0	374	374	-53.8292
Mass Density (kg/m <sup>3</sup> )	815.745	955.148	955.148	291.265
Liquid Compressibility (cP)	1.65731 ×10 <sup>6</sup>	5.17427 ×10 <sup>7</sup>	5.17427 ×10 <sup>7</sup>	1.65731 ×10 <sup>6</sup>

Oil Volumetric Formation Factor  $\beta_o$  (a) and density  $\rho$  (b) curves that were used in the models are shown in figure 5.

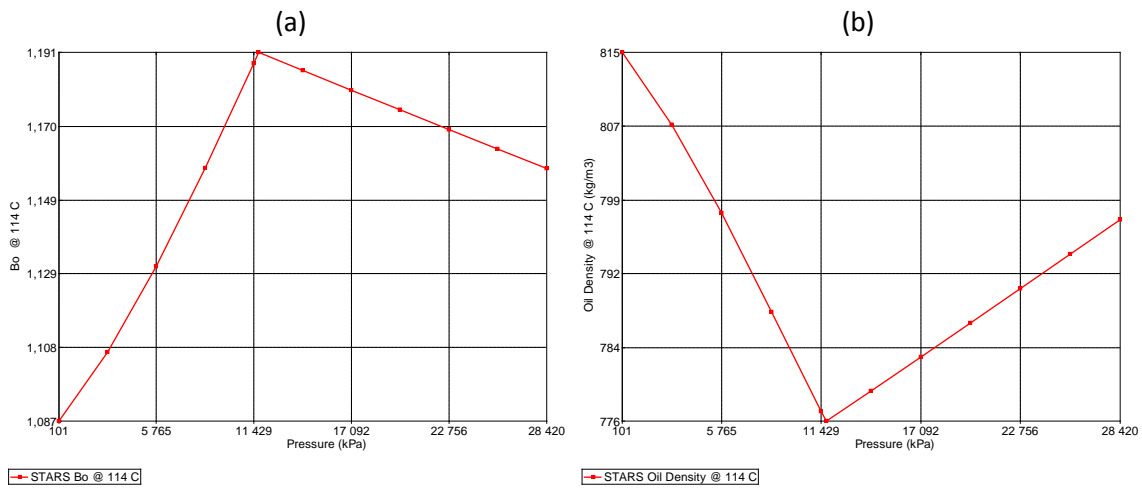


Figure 5. Oil volumetric formation factor (a) and density (b) vs pressure.

Oil viscosity used in the models is shown in figure 6 for Reference Temperature (a) and Reference Pressure (b).

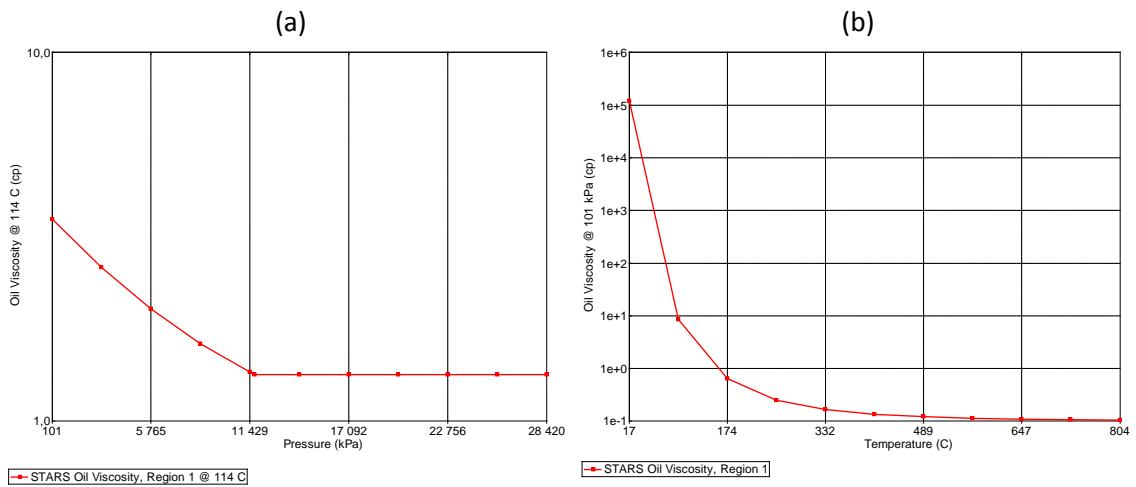


Figure 6. Oil viscosity vs pressure (a) and temperature (b).

Relative Permeability curves used in the model are shown in figure 7.

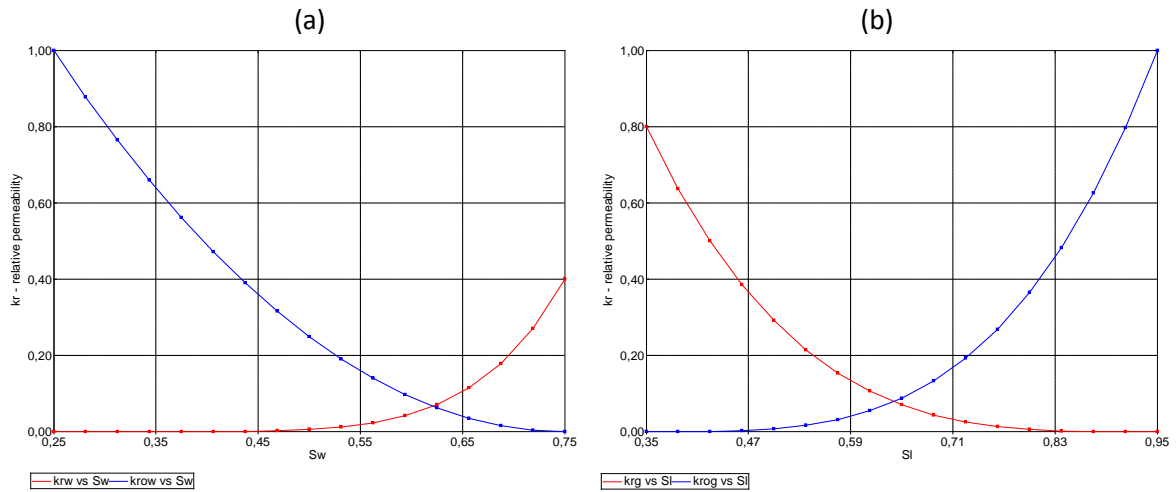


Figure 7. Relative permeability curves for water (a) and liquid (b).

Most of the models have the same well definitions and production/injection schemes. Table 4 contains the most important parameters for the simulation of the models.

Table 4. Well definitions and schemes used in the models.

	Injector	Producer
Type	Sink/Source	Flexwell
Name	INJE-1	PROD-1
Perforation Positions	14 6 1	2 6 1
	14 6 2	2 6 2
	14 6 3	2 6 3
	14 6 4	2 6 4
	14 6 5	2 6 5
Wall ID (m)	0.15	0.130
Wall OD (m)	NA	0.152
Cement OD (m)	NA	0.200
Wall Heat Capacity	NA	$3.630 \times 10^6$ J/(m <sup>3</sup> *°C)
Wall Heat Conductivity	NA	$3.888 \times 10^6$ J/(m*day*°C)
Cement Heat Capacity	NA	$1.848 \times 10^6$ J/(m <sup>3</sup> *°C)
Cement Heat Conductivity	NA	$1.184 \times 10^5$ J/(m*day*°C)
Injected fluid temperature	15 C	-
Maximum Bottom-hole Pressure	40000-45000 kPa	20000 kPa
Maximum Injection Rate	1000-2000 m <sup>3</sup> /day	
Maximum Production Rate		1000 m <sup>3</sup> /day

Simulation starts on 01/26/1987 with a Water Upper Injection Rate Limit of 1000 m<sup>3</sup>/day until 01/25/1998 (notice the reservoir has been waterflooded during several years prior to cases study) when the injected fluid is switched to Tracer (aqueous), with an Upper Injection Rate Limit of 2000 m<sup>3</sup>/day, this to generate an injection boost and measure how the temperature and tracer behave during this period of two days until 01/27/1988, when injection is changed back to initial conditions (Water as the Injected Fluid and Upper Injection Rate Limit of 1000 m<sup>3</sup>/day).

This boost in injection rate is precisely done in order to evaluate how temperature pulse reaches the producer well and also to compare the time with the aqueous tracer's flight time.

## 4.2. Models

Several simulations were run in order to assess a link between reservoir characteristics and temperature responses. The cases evaluated included homogeneous, heterogeneous, Dykstra-Parsons (DP) variations, channel and fracture. These will be discussed below.

### 4.2.1. Homogeneous Model

The model is consistent with those properties presented before, in addition, the permeability and porosity are constant across the whole model with values of 210 mD and 0.3 respectively. Figure 8 is taken from *Builder* and shows the permeability in x-direction of the homogeneous model.



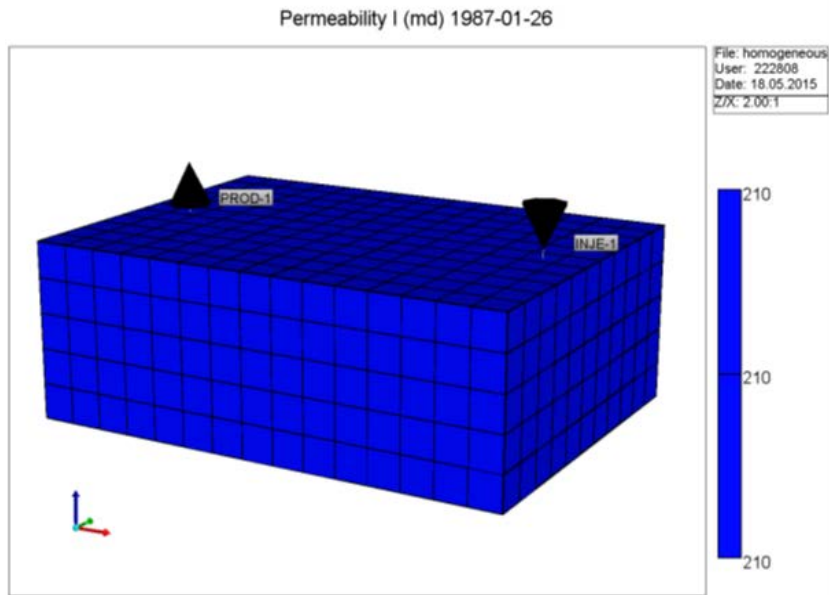


Figure 8. Homogeneous model showing permeability in x-direction.

#### 4.2.2. Heterogeneous Model

In this model, the main change is in permeability, for the construction of this models different arranges were evaluated and permeability values per layer that were used are: 40 for layer 1, 1000 for layer 2, 5 for layer 3, 3 for layer 4 and 1 for layer 5 (shown in Figure 9). This model can also be evaluated as a thief zone. Particularly, in this model is also evaluated the under- and over-burden effects on the temperature response.

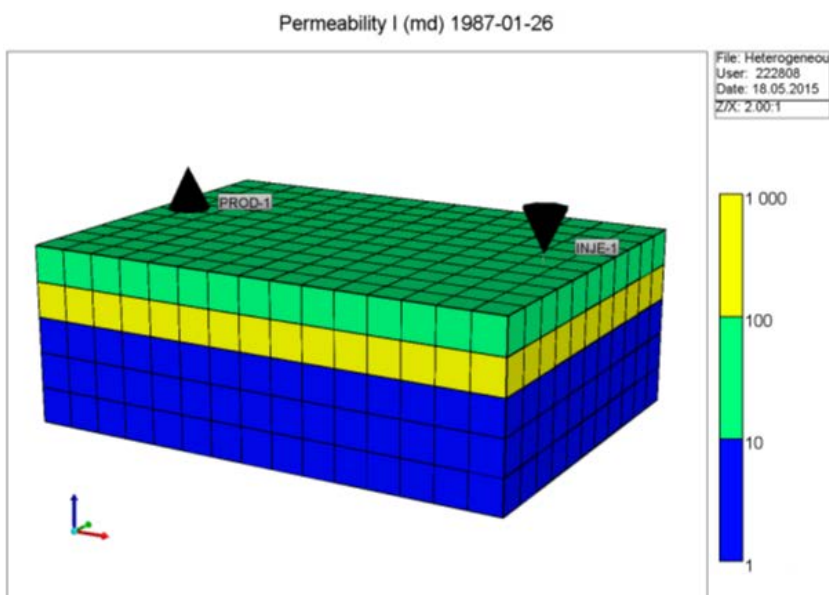


Figure 9. Heterogeneous model showing permeability in x-direction.

### 4.2.3. Dykstra-Parsons Variation Models

In order to evaluate how permeability heterogeneities (by layer) can affect the results, 4 models were performed with different Dykstra-Parsons coefficients, being these 0, 0.2, 0.5 and 0.98 (shown in figure 10).

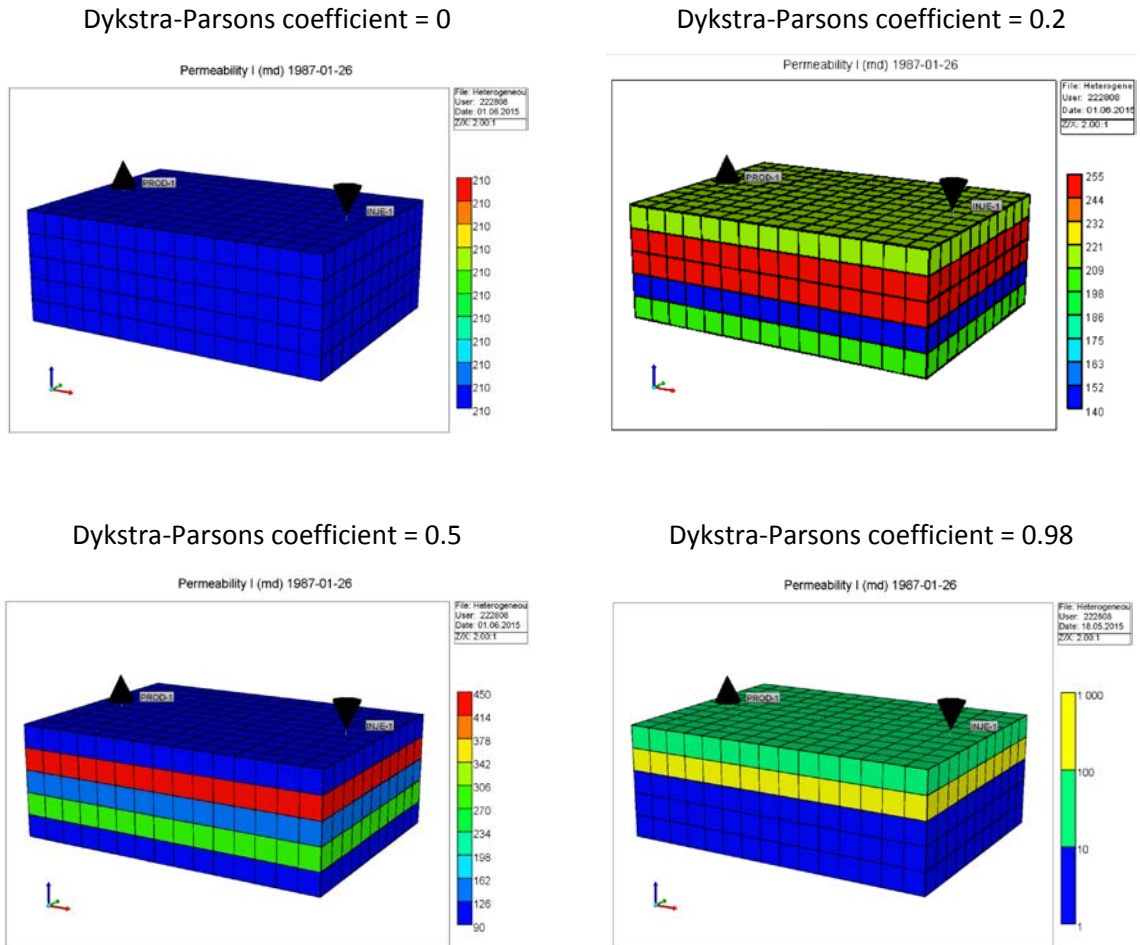


Figure 10 Dykstra-Parsons models showing permeability in x-direction.

### 4.2.4. Channel Model

A channel is defined to have the same porosity as its surroundings but with a higher permeability. Two models were evaluated; one having constant permeability in the surroundings and the other with varying permeability. For both models, porosity was set to 0.3. Figure 11 shows the permeability in x-direction for the channel model with varying permeability.

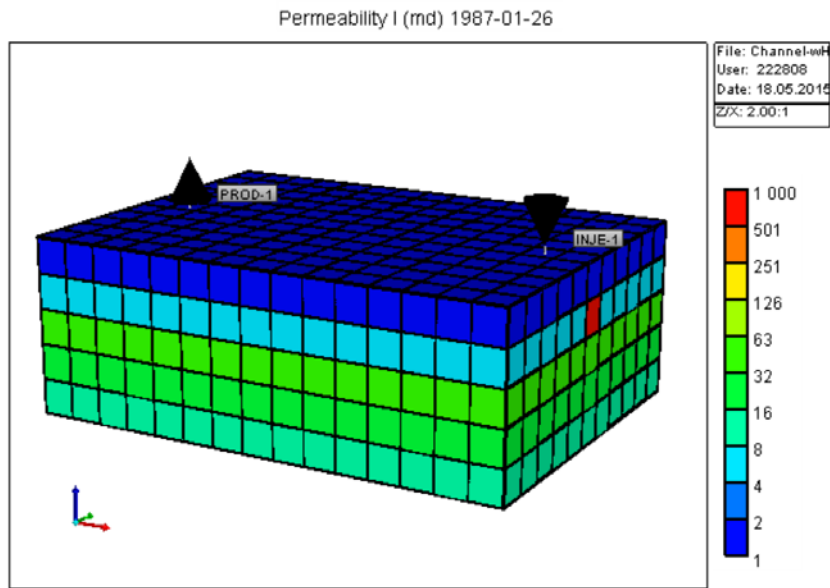


Figure 11. Channel model showing permeability in x-direction.

#### 4.2.5. Fracture Model

For this model, both permeability and porosity vary. This model was performed for different scenarios, with porosity variations within the fracture. Porosity were 0.003, 0.01, 0.02, 0.03 and 0.05. Afterwards, it will be discussed why these values. Figure 12 shows the permeability in x-direction for the fracture model with porosity of 0.003 in the fracture.

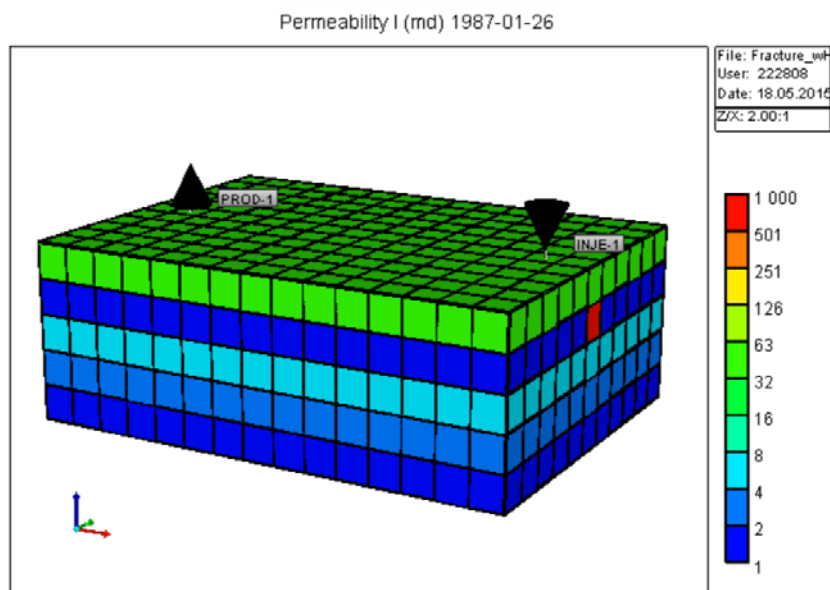


Figure 12. Fracture model ( $\Phi$  0.003) showing permeability in x-direction.

## 5. Results and Analysis

After running and evaluating several simulations, all cases were completed and the results are presented in this chapter.

### 5.1. Influence of Heat Losses in Over-/Underburden and Heterogeneity

The homogeneous case was compared with the heterogeneous on terms of under and over burden heat losses, figure 13 shows result screenshots for temperature profile after 10 years of water injection.

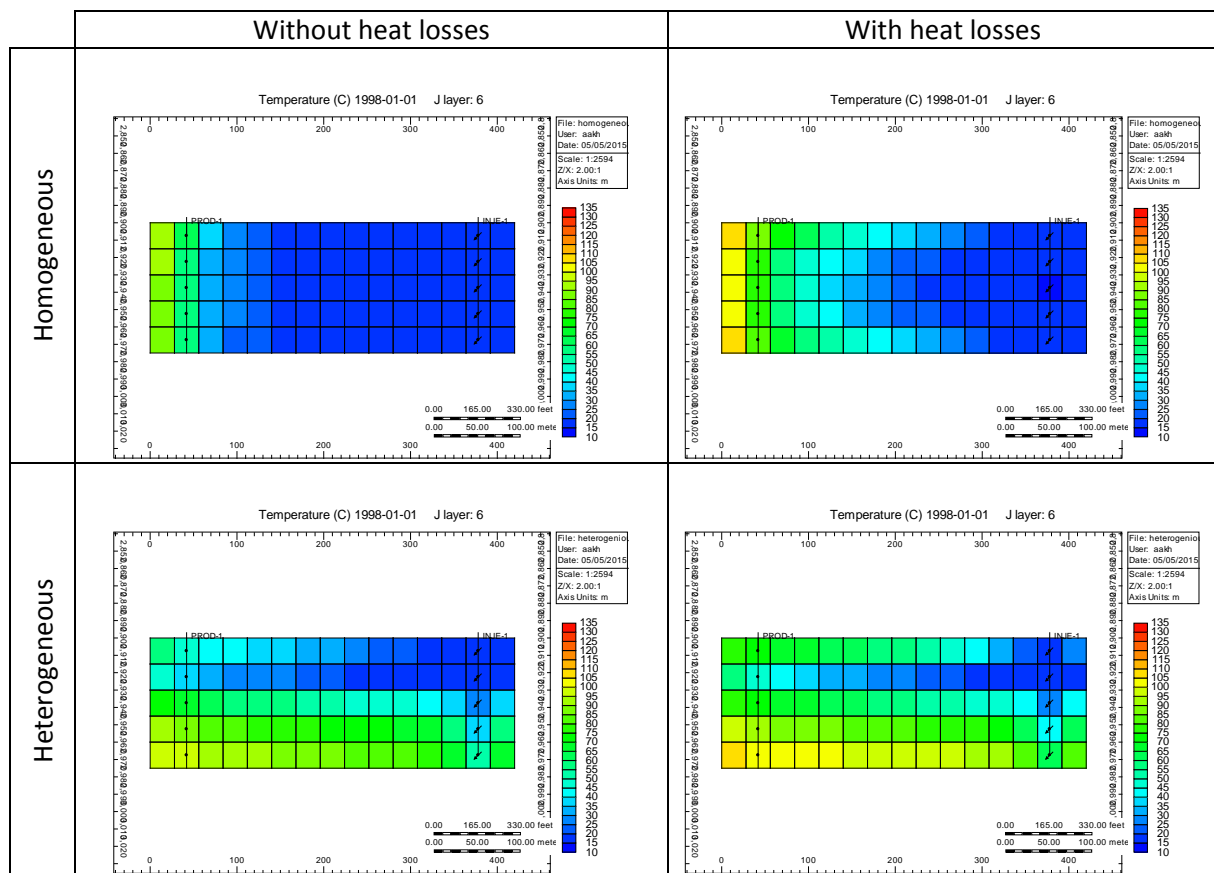


Figure 13. Effects of heterogeneity and heat losses (over-, underburden) to resulting temperature distribution in cross-section between the producer-injector pair.

It is easily noticeable that for the homogeneous case without heat losses, the temperature front moves homogeneously throughout the reservoir, but when heat losses are accounted then there's a curved front due to the heat transferred from upper and lower boundaries. When heterogeneous case is run it is found that the layers with higher permeability, by allowing higher flow of water through them,

cool down faster than the rest of the reservoir. Here once again it can be noticed how when including heat losses from under and over burden, the cooling down of the top and bottom layers retracts.

Since it is shown how important is to take into account under- and overburden heat losses, following simulations were performed accounting for heat losses.

### 5.2. Temperature Response of the Homogeneous Model

The main objective of this work is to evaluate the temperature response in the producing well, under different geometry schemes. For the model with constant permeability and porosity throughout its boundaries, the temperature response is shown in figure 14; during the whole production period.

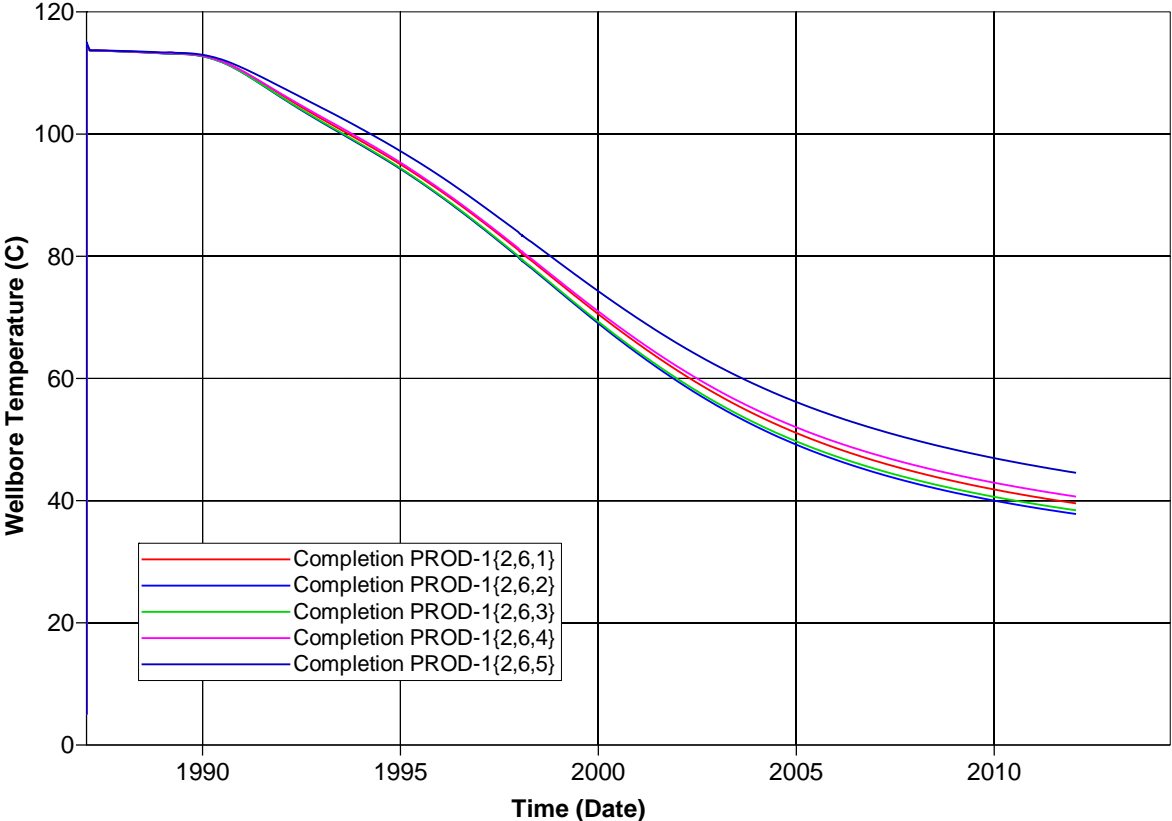


Figure 14. Temperature sensing for the homogeneous model.

As it can be observed, there is not any special signal that the producer is getting some response for the temperature boost and this is because of the reservoir’s homogeneity. Figure 15 shows a close up to the boost period for the homogeneous case; highlighted is the two days boost period.

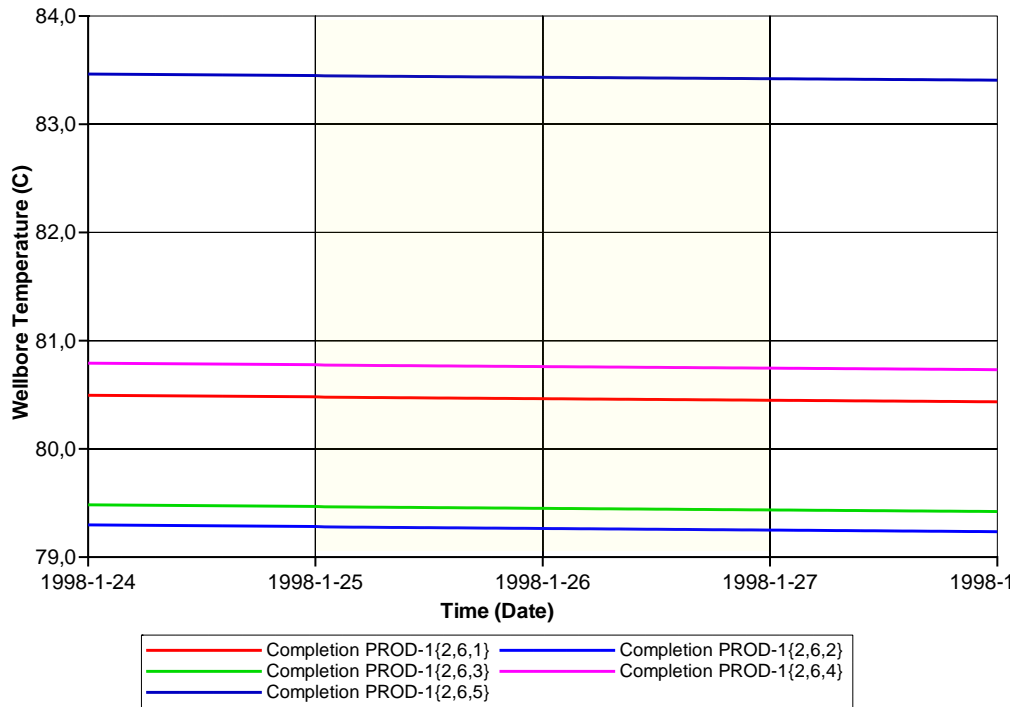


Figure 15. Temperature sensing during injection boost for the homogeneous model.

Figure 16 shows the temperature reading for the wellbore (FLEXWELL) and reservoir (block temperature) at the end of the injection boost. This distinction between both readings is the main reason FLEXWELL model is used to better modeling temperature instead of using a conventional sink/source model. The FLEXWELL temperature reading represents a sensor inside the wellbore.

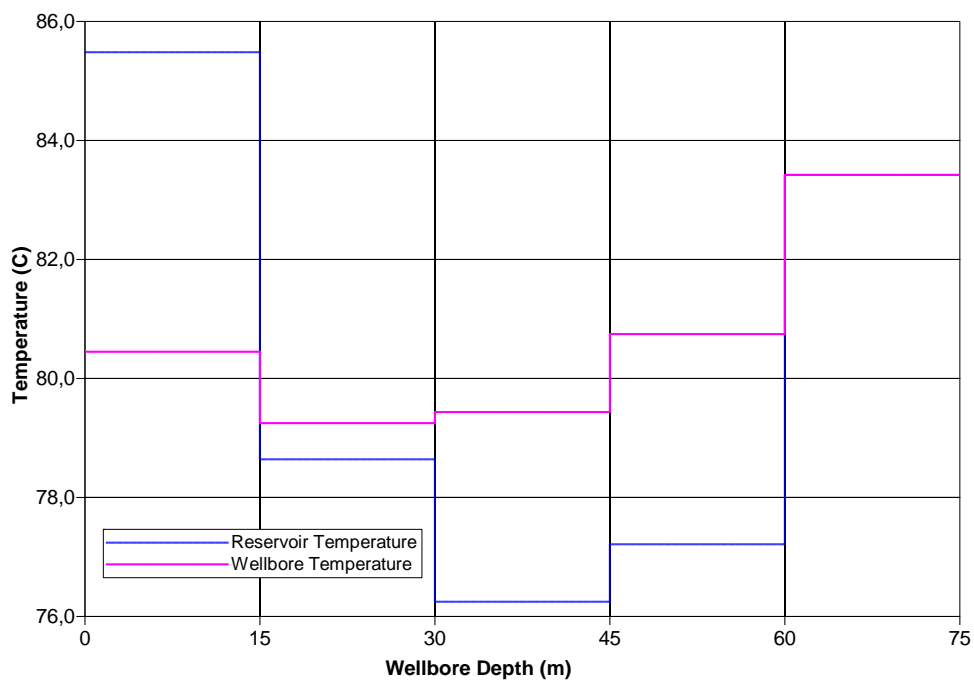


Figure 16. Temperature readings in the wellbore (FLEXWELL) and reservoir (block temperature) at the end of the injection boost for the homogeneous model.

### 5.3. Temperature Response of the Heterogeneous Model

The heterogeneous case has a high permeable layer, this can be seen as a thief zone. The results for the temperature profile are shown in figure 17.

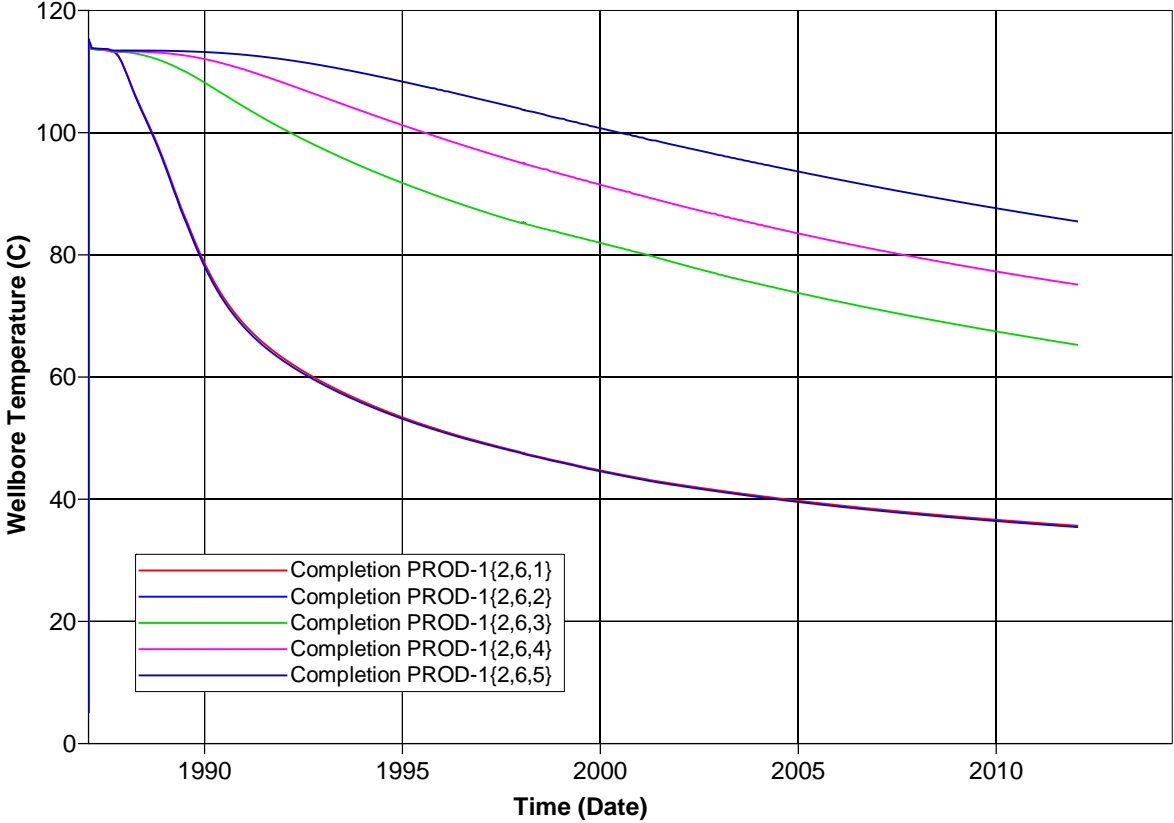


Figure 17. Temperature sensing for the heterogeneous model.

In this case, we can notice that layer one is also sensing the temperature response coming from layer two, since that’s how the gauge inside the FLEXWELL model works. Layer two, having a permeability of 1000 mD, gives a quicker response to the producer, likewise, the temperature drop in this layer is higher than the others.

Figure 18 shows a close up for temperature response and injection rate during the injection boost period. It can be seen that the temperature response is not that evident, afterwards this will be discussed. Figure 19 shows the temperature reading for the wellbore (FLEXWELL) and reservoir (block temperature) at the end of the injection boost.

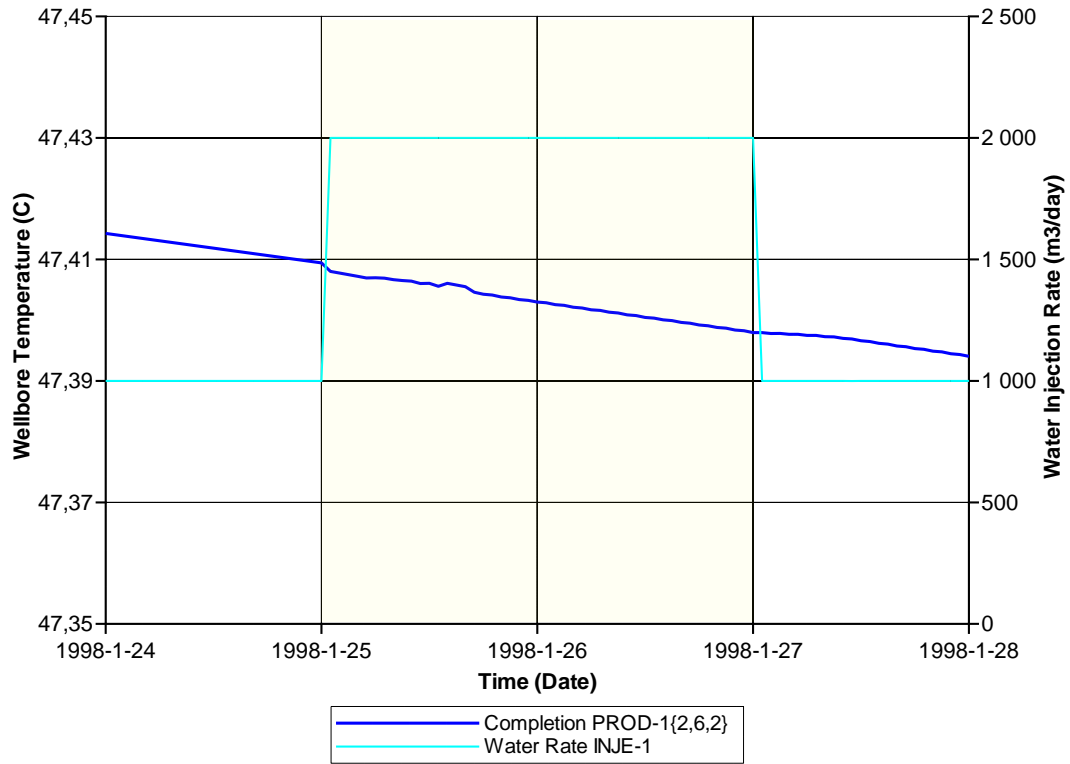


Figure 18. Temperature sensing for completion (2,6,2) during injection boost for the heterogeneous model

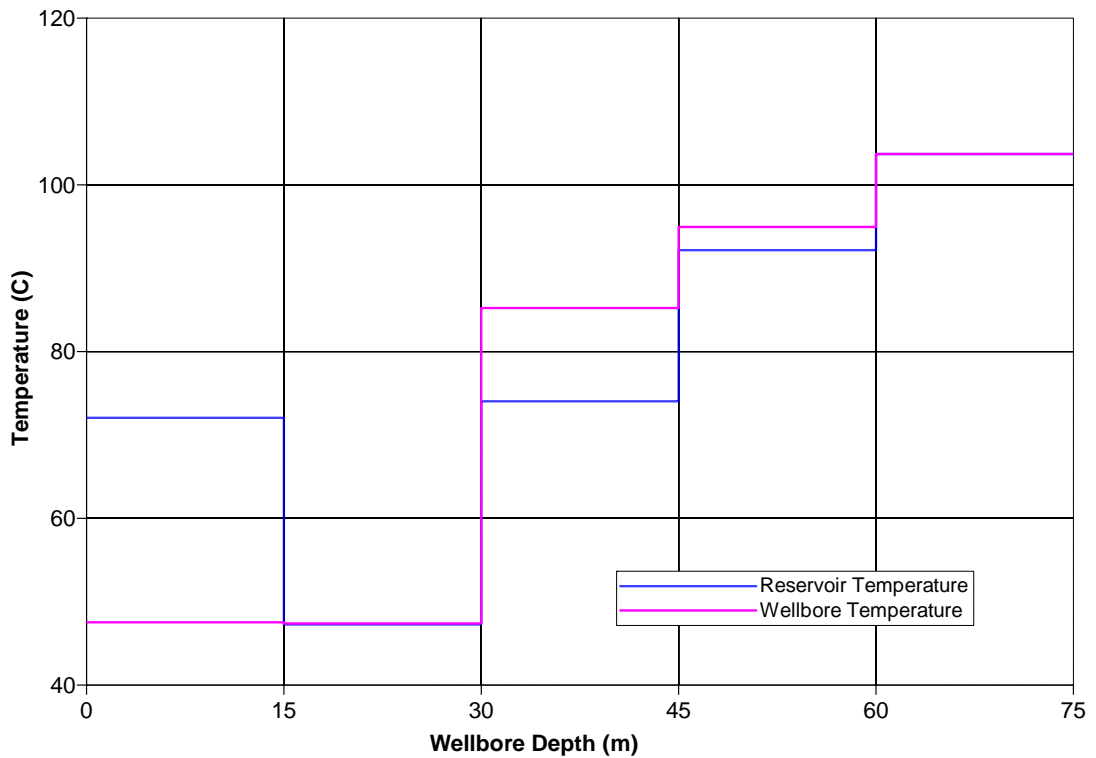


Figure 19. Temperature readings in the wellbore (FLEXWELL) and reservoir (block temperature) at the end of the injection boost for the heterogeneous model.



## 5.4. Temperature Response for the Dykstra-Parsons Variation Models

Reservoir heterogeneities are infinite, a reservoir can present several configurations along its length, in order to check the permeability influence in the use of temperature as a tracer four cases were evaluated. Table 5 shows the permeability variation in the x-direction for each case.

Table 5. Permeability for the Dykstra-Parsons variation models.

	DP coefficient = 0	DP coefficient = 0.2	DP coefficient = 0.5	DP coefficient = 0.98
Layer 1	210 mD	210 mD	90 mD	40 mD
Layer 2	210 mD	255 mD	450 mD	1000 mD
Layer 3	210 mD	245 mD	130 mD	5 mD
Layer 4	210 mD	140 mD	280 mD	3 mD
Layer 5	210 mD	200 mD	100 mD	1 mD

For these configurations, temperature profiles after 10 years of water injection are shown in figure 20.

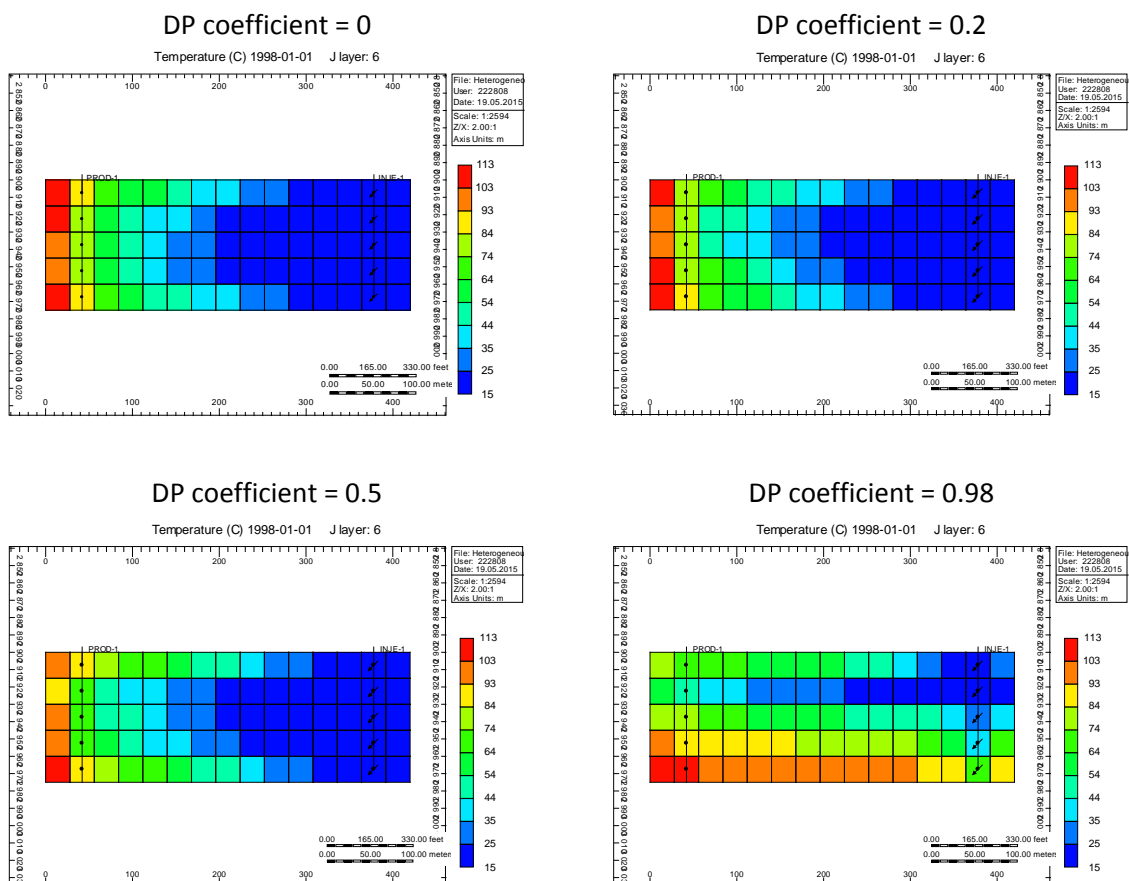


Figure 20. Temperature distribution in cross-section between the producer-injector pair for Dykstra-Parsons variation models.

Here, once again we can evidence how the permeability plays an important role on the temperature front displacement, i.e. the higher the permeability, the greater the temperature change through the pair of wells.

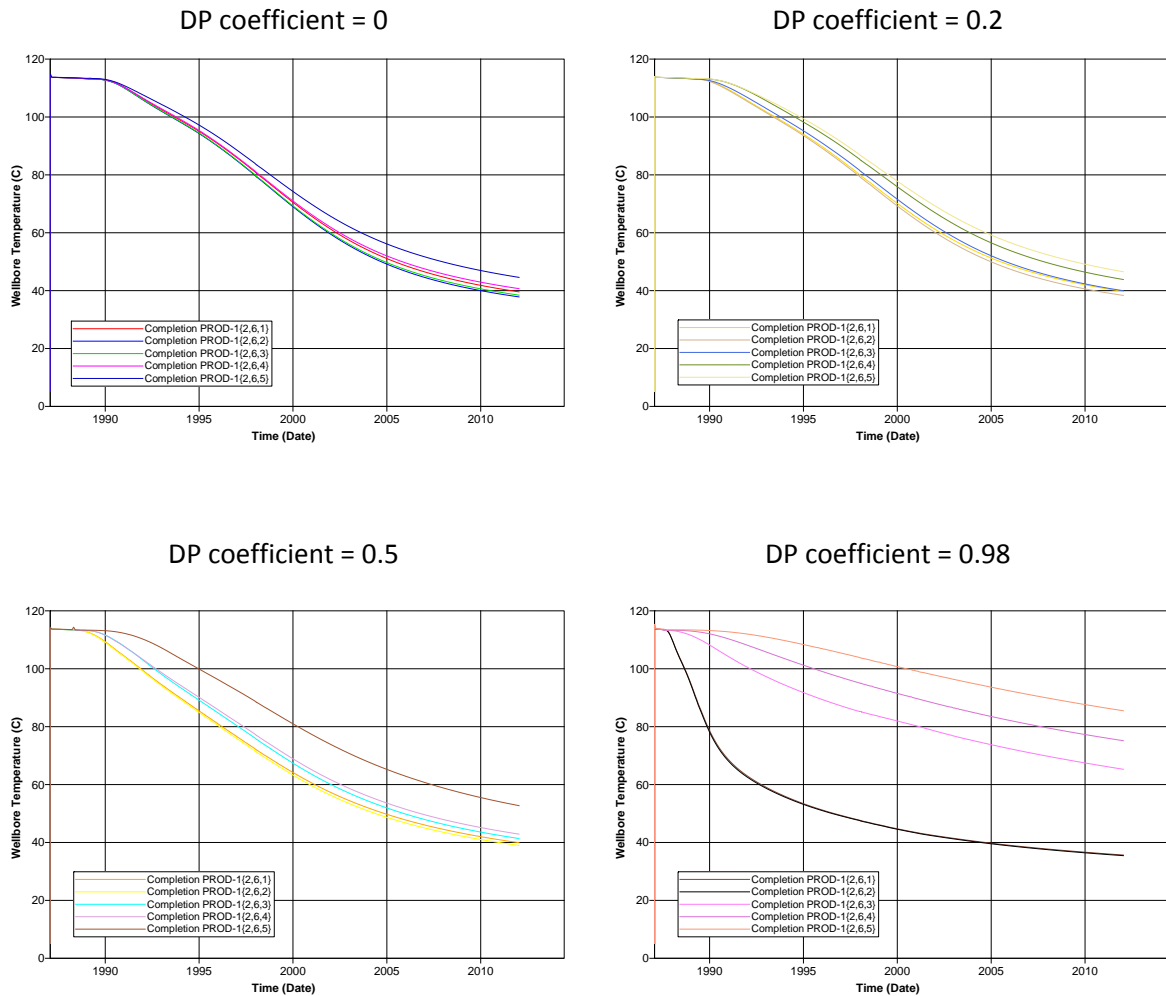


Figure 21. Temperature sensing for the Dykstra-Parsons variation models.

In figure 21 it gets more evident how the permeability plays an important role on the temperature behavior, i.e. the higher the permeability the bigger the temperature drop and different behavior from those with smaller permeability.

### 5.5. Temperature Response of the Channel Model

The channel model temperature distribution is shown in figure 22 for all layers, after 10 years of injection. In this case, the channel is in layer 2, connecting both the injector and producer well pair. It is therefore, as expected, that the completion (2,6,2) gets a quicker and greater response than those no channel-connected.

Temperature (C) 1998-01-01 J layer: 6

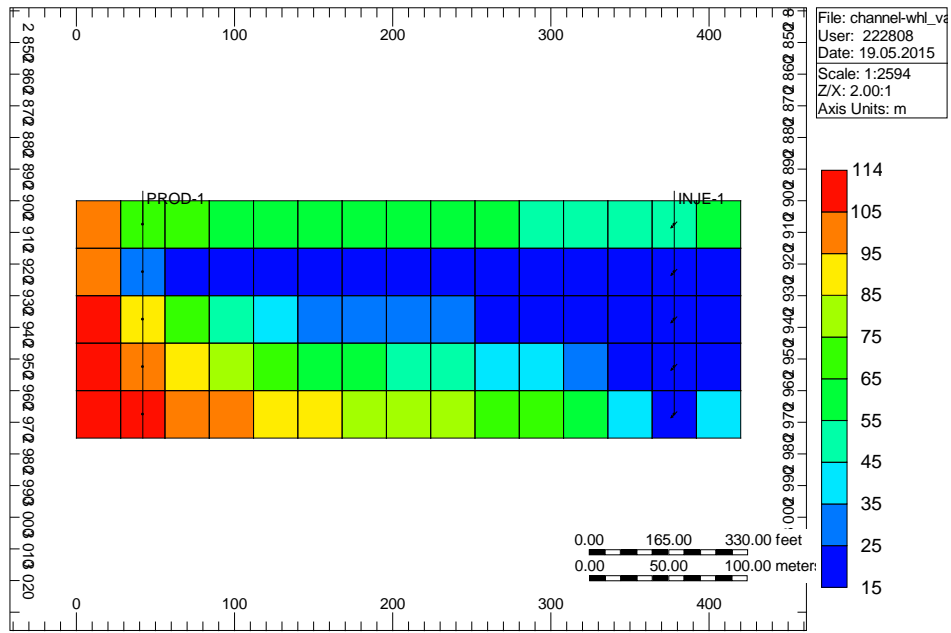


Figure 22. Temperature distribution for the channel model.

The temperature sensing profile for all layers is shown in figure 23, in this model, the layer 2, which has the higher permeability, presents a clear response to the injection boost.

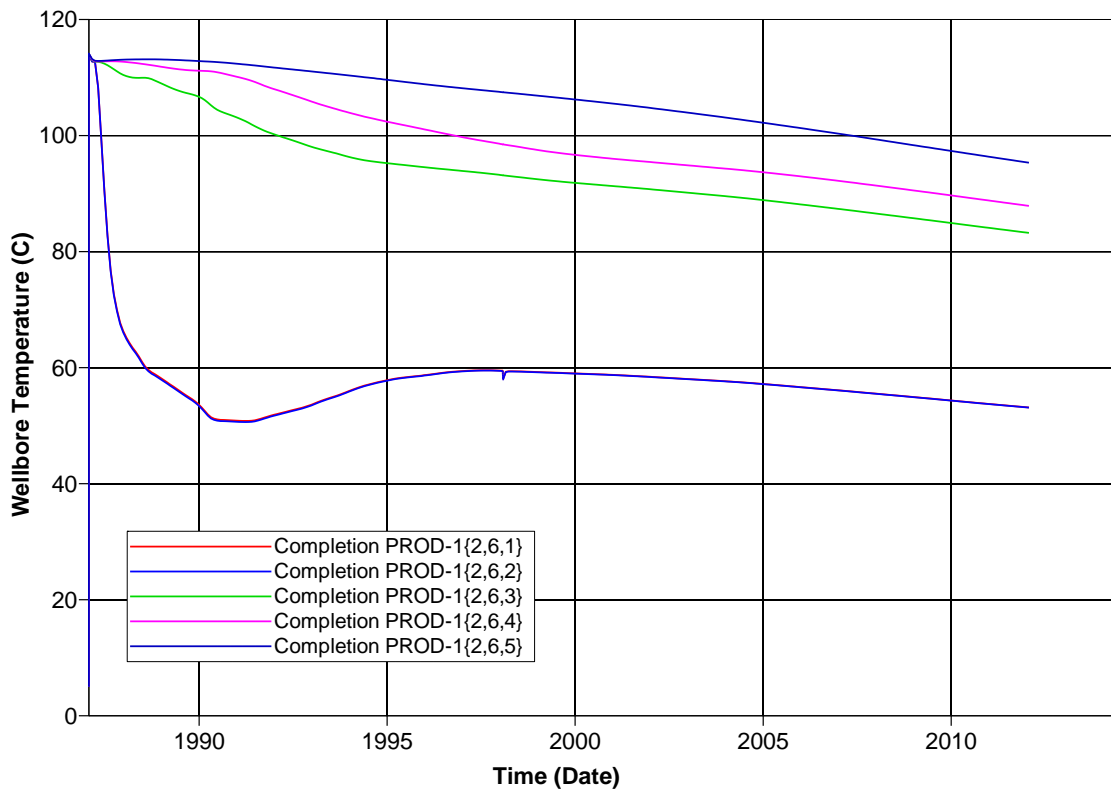


Figure 23. Temperature sensing for the channel model.

Close up to the injection boost and temperature readings are shown in figures 24 and 25, it is noticeable that the time for the trend to be back to previous one again is quite large, however, the response is quite quick.

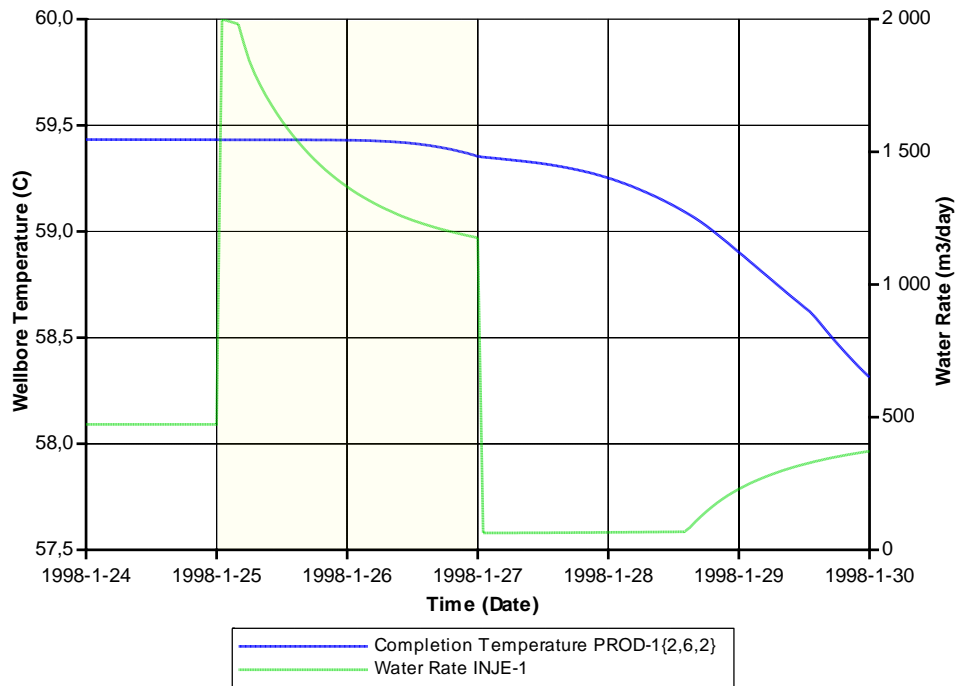


Figure 24. Temperature sensing for completion (2,6,2) during injection boost for the channel model.

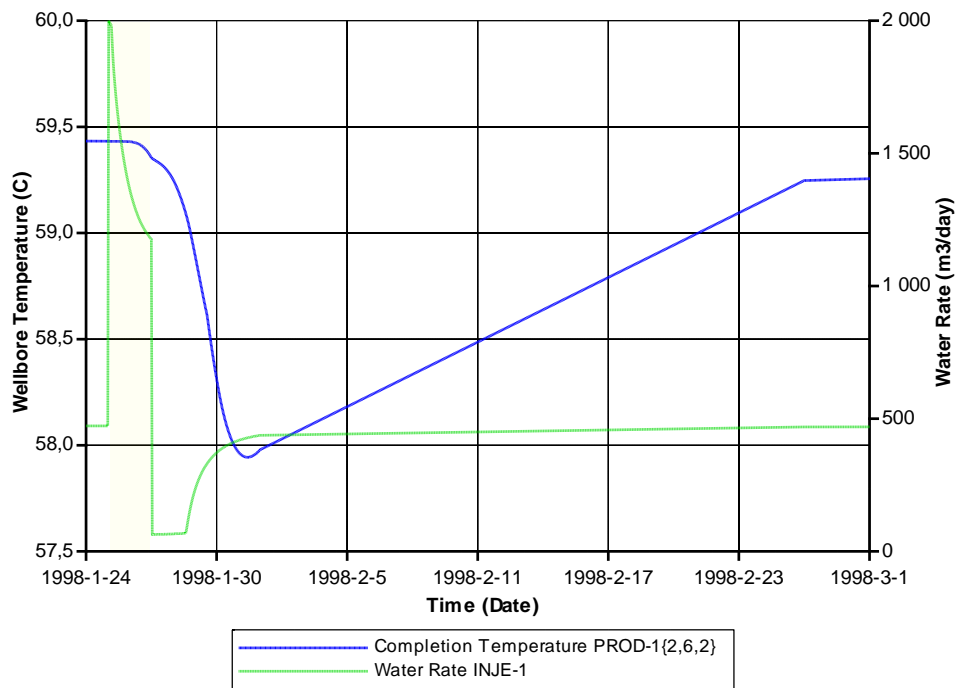


Figure 25. Temperature sensing for completion {2,6,2} during temperature response time for the channel model.

In figure 26 it is shown the amplitude and response time of the temperature after the injection boost for the channel model. Orange dotted line shows how the temperature would behave if no injection boost were applied.

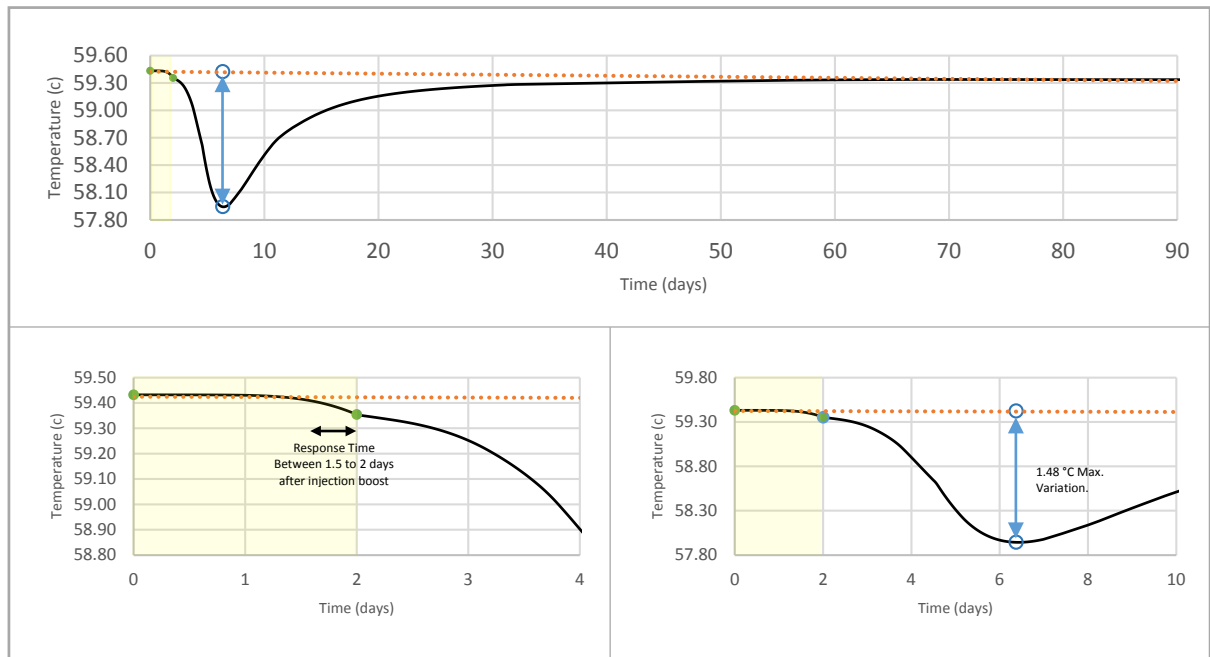


Figure 26. Temperature response for layer 2. Showing temperature response after the injection boost period, time of response and maximum temperature drop due to the boost, for the channel model.

Figure 27 shows the response time for the tracer in the channel model. It is about after 36 days when the tracer arrives the production well for this case.

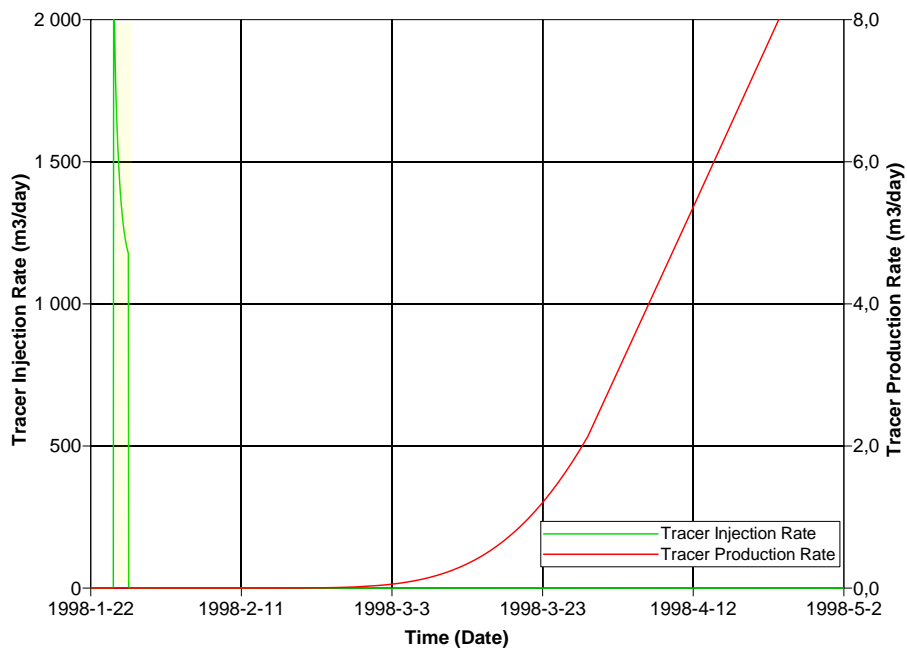


Figure 27. Tracer arrival time for the channel model.

## 5.6. Temperature Response of the Fracture Models

After evaluating several cases and taking into consideration the results from previous models, the next models to discuss are those with a fracture. For the fracture case, it was evaluated for different porosities within the fracture; since it seems to have a great impact on the temperature response. Figure 28 shows the temperature response for all different cases.

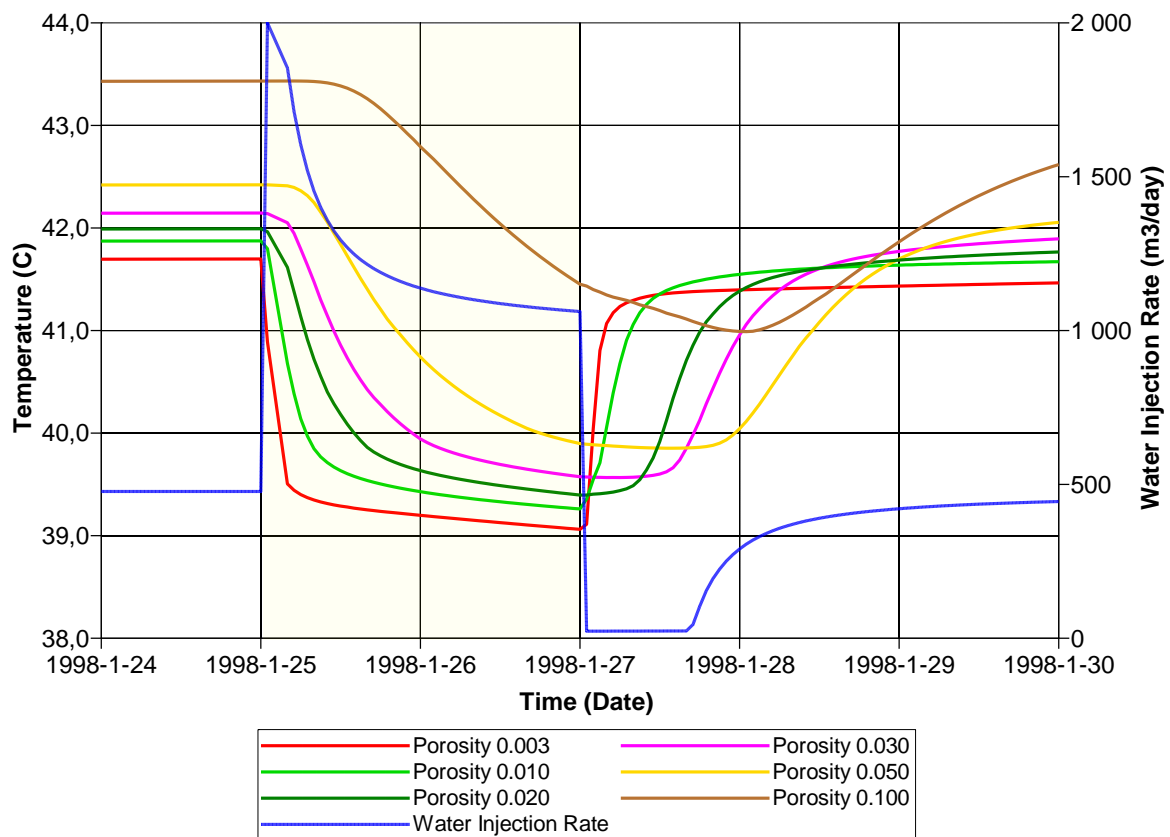


Figure 28. Temperature sensing for fracture model with different porosity.

In figure 28 it is notable that the fracture with the smaller porosity results in a quick and larger temperature response for both configuration; injection boost start and end. The trend goes to the case with the biggest porosity where the temperature response occurs later after the injection boost, the temperature continue declining for a longer period than those with smaller porosity.

It is worth noting that the simulator temperature gauge measures the temperature in the well stream and therefore the result is influenced by those temperatures coming from lower producing layers. Nevertheless, the result in the temperature wave is evident and can be observed from the layer affected (e.g. by the fracture) and upper layer gauges.

Figure 29 shows the temperature sensing for the case with porosity 0.003 within the fracture. Figure starts from the start of the injection boost period (highlighted). The orange line denotes the trend the temperature would follow if no injection boost were introduced, for this case, a temperature response is seen in less than 2 hours and the amplitude of the response (maximum temperature deviation) is of 2.77°C after 2 days. The temperature build-up starts after 49 hours; just one hour after decreasing injection pressure back.

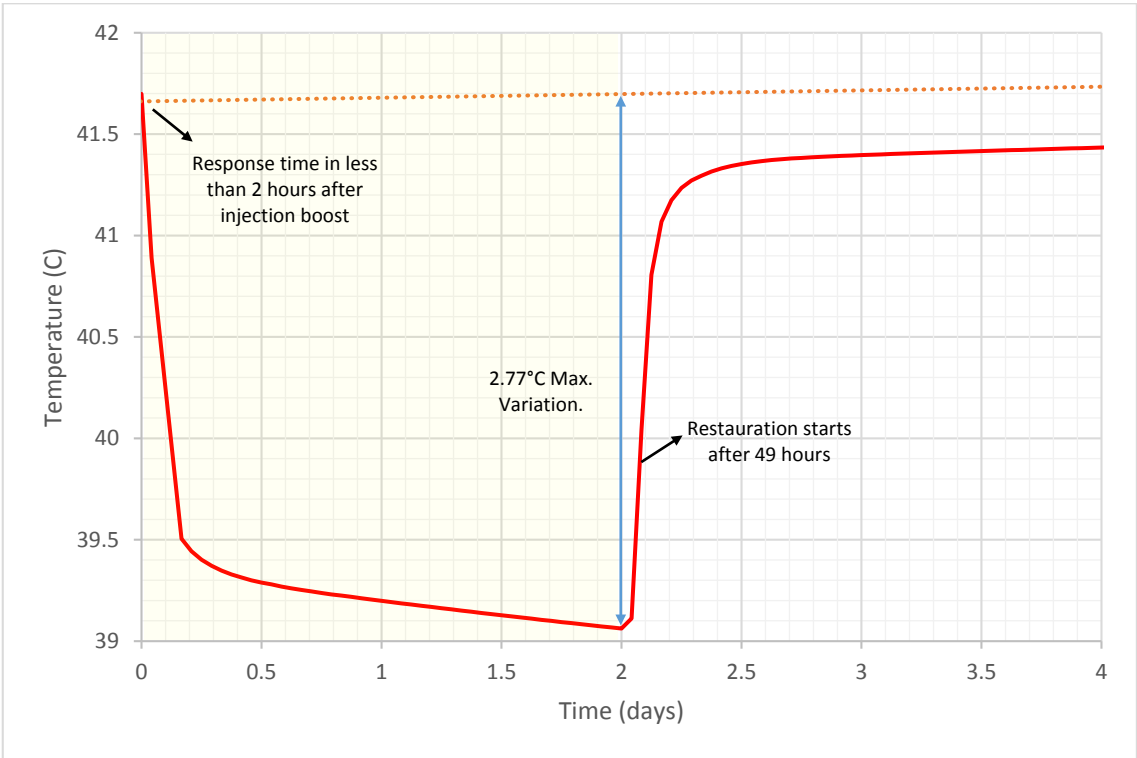


Figure 29. Temperature sensing for fracture model with porosity of 0.003 within the fracture.

Figure 30 shows the temperature sensing for cases with porosity of (a) 0.01, (b) 0.02, (c) 0.03 and (d) 0.05. For the case with 0.01, a temperature response is seen between 3 to 4 hours from boost start, the amplitude of the response is of 2.66°C and the restauration starts after 50 hours. For the case with 0.02, a temperature response is seen between 4 to 5 hours, the amplitude of the response is of 2.65°C and the restauration starts after 56 hours. For the case with 0.03, a temperature response is seen between 5 to 6 hours, the amplitude of the response is of 2.63°C and the restauration starts after 63 hours. For the case with 0.05, a temperature response is seen between 7 to 8 hours, the amplitude of the response is of 2.61°C and the restauration starts after 70 hours. A clear trend is evidence here where with bigger porosity within the fracture, the slowest the response, the lowest the amplitude and the latest the restauration kick off.

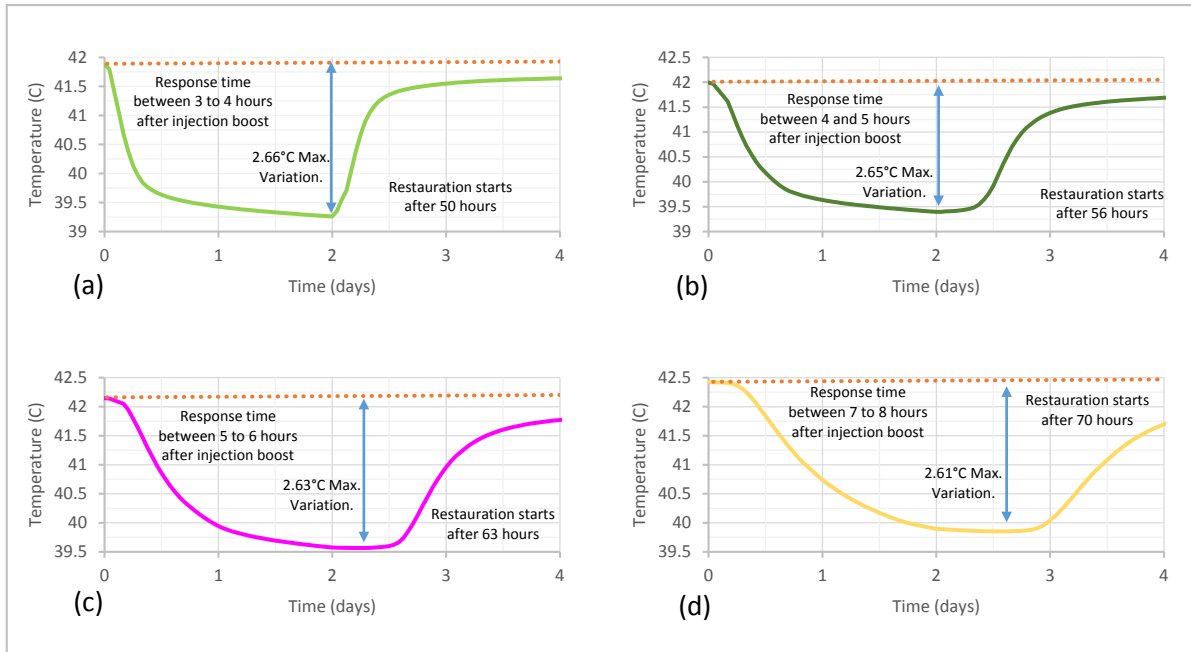


Figure 30. Temperature sensing for fracture cases with porosity of (a) 0.01, (b) 0.02, (c) 0.03 and (d) 0.05 within the fracture.

In figure 31 the results for the case with 0.1 porosity are presented. Having the largest porosity evaluated, this case shows a temperature response between 12 to 13 hours, the amplitude of the response is of 2.48°C and the restoration starts after 80 hours. Here, the trend is the same as before, having a higher porosity, the temperature response is slower and when the porosity goes to 100%, no response will be obtained.

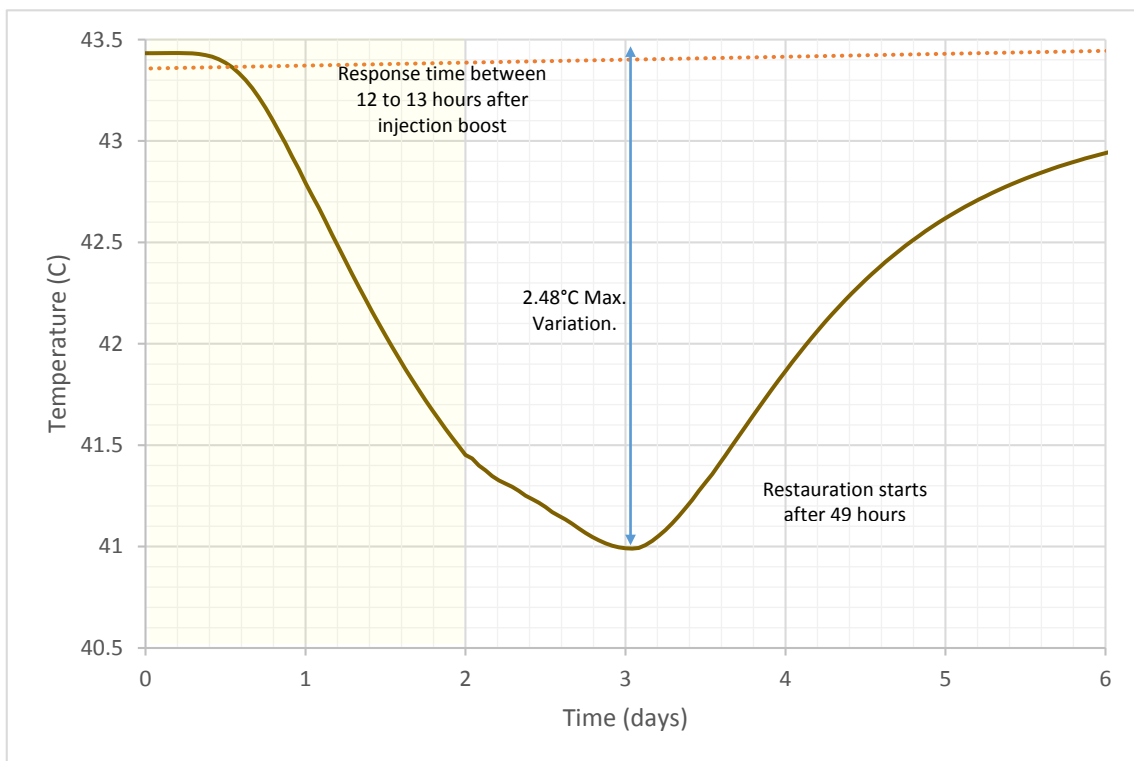


Figure 31. Temperature sensing for fracture model with porosity of 0.1 within the fracture.



Figure 32 shows the behavior of the temperature front when the permeability is varying as (a) 250mD, (b) 500 mD and (c) 750mD from the injection boost start. It can be observed how permeability restricts the temperature flow through the fracture, the lower the permeability the lower the temperature drop across the whole production period and response amplitude during the injection boost.

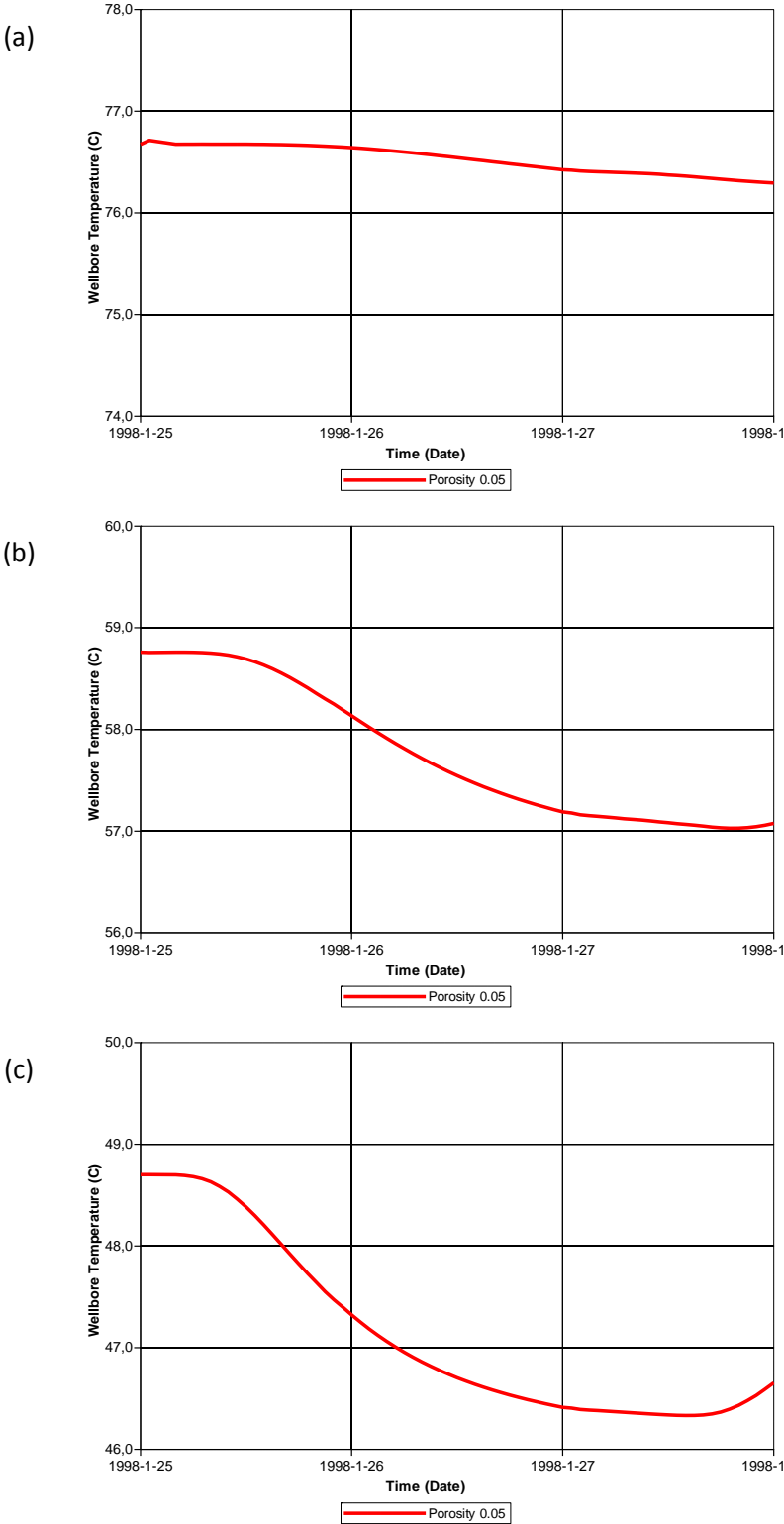


Figure 32. Temperature sensing for permeability variations of (a) 250mD, (b) 500 mD and (c) 750mD in the 0.05 porosity fracture model.

Figure 33 shows the Tracer production for the fracture cases, here, as with temperature, the porosity plays an important role on the arrival time, being faster for the smaller porosity and slower (to almost untraceable) when the porosity increase.

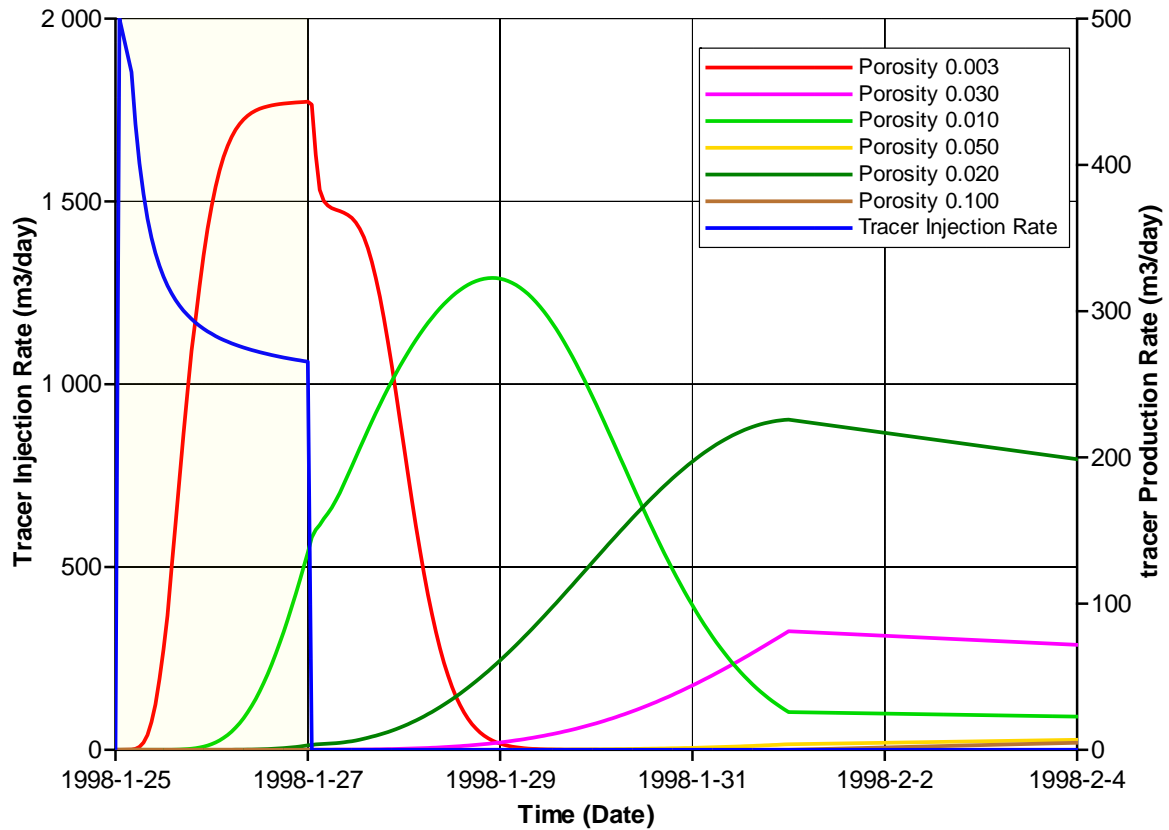


Figure 33. Tracer production rates for the fracture case with different porosities.

Both temperature and aqueous tracers are introduced in the reservoir at the same time, since the cold water injection boost, in this date is treated as the aqueous tracer (i.e. 100% of water injected is specified as “tracer” in the simulator), this was done in order to compare the efficiency between both methods; specifically in terms of time. Figure 34 is a comparison for the arrival times between temperature and an aqueous tracer, the figure starts from the injection boost start and it is observable that the temperature response (in orange) is sensed before the aqueous tracer (in blue) for all the cases.

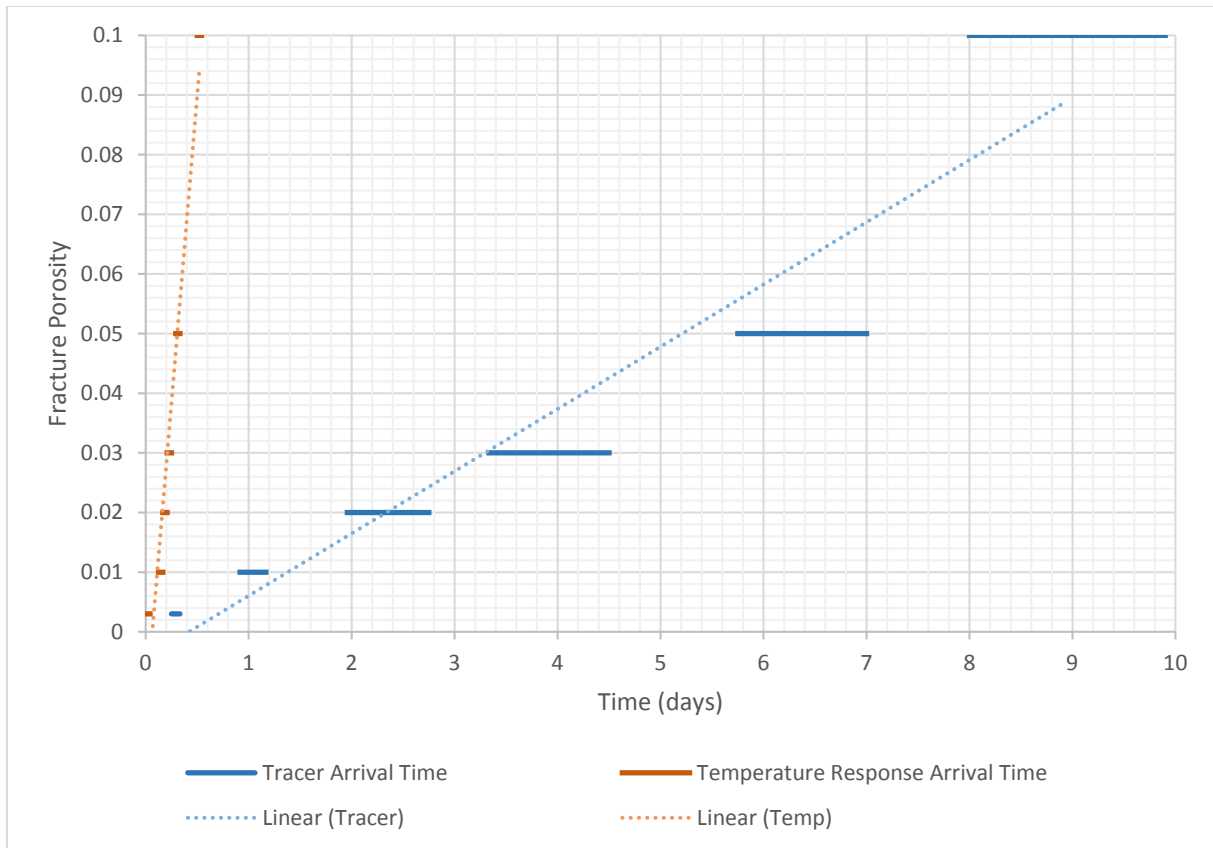


Figure 34. Comparison between temperature and tracer arrival times for the fracture model with different porosities.

From figure 34 it seems to be a correlation between arrival times of temperature and chemical tracer for different porosities, from the simulations performed it was obtained that the aqueous arrival time is about ten times greater than the temperature arrival time for porosity increase, i.e. the difference between temperature and aqueous trace arrival times for porosity of 0.01 increases ten time for porosity of 0.1 and the same for porosity of 0.003 against porosity of 0.03.

## 6. Conclusions

The following conclusions were obtained:

It is very important to stress that for non-isothermal modeling, under- and over-burden heat losses must be accounted, since they help to better characterize the behavior of the temperature front in the reservoir; neglecting of heat losses may lead to significant errors.

The temperature transient effect or temperature response in the producer is affected by the permeability and porosity of the high permeable feature connecting injector producer well pair: Higher permeability leads to faster temperature front movement and smaller porosity results in larger response drop.

Downhole temperature measurements may be used to identify certain types of reservoir heterogeneities such as a connecting fracture or high permeable channel. For all the cases where a feature (channel or fracture) was introduced, a boost in cold water injection rate generated a temperature transient effect across the reservoir and, according to the reservoir properties, this drop is highly probable to be observed in the producing well.

- In the case of thief layer, the temperature response was not much evident.
- In the case of channel, the response was relatively slow. It took days to be sensed and the drop lasted for several days after the boost stopped until it reached equilibrium again. In this case the temperature response is longer than when a fracture is present but still is faster than an aqueous tracer.
- When a fracture is present, this method is particularly effective; the response is very sensitive to the fracture pore volume. Also, for these cases the temperature response time is faster about ten times compared to an aqueous tracer.

From the previous points it can be concluded that the temperature response is a result of a complex interplay between porosity and permeability which seems to be similar to that of pressure transient effects. The link between pressure and temperature transient effects is a subject of future work.

Analysis of temperature transient effects may be very useful to support decision making for EOR methods deployment (low salinity, surfactant flooding, polymer flooding, gel treatment, etc.) and help to improve its efficiency.

## 7. Limitations and Future Works

When dealing with reservoir simulation, sometimes simpler is better, especially when a result is needed in a short time or to evaluate several configurations. Also, the CMG University License only allows a certain amount of blocks for the models, therefore a finer grid model could not be done.

Results presented here are based in numerical simulation runs and are therefore linked to how the simulator handles different properties, in the field, the behavior of a reservoir can be different, (however, the constant research and updates on numerical techniques makes this breach shorter), it would be of utmost importance to upscale this research to a field level that allows to better understand the behavior of temperature in the reservoir.

In this work different features connected from side to side to the well injector and producer pair were studied, it will be relevant to study the behavior of temperature when such features are not connected to the wells or have different directions.

Finally, these features may present infinite configurations in terms of density, flux direction, connectivity, among others that will be worth to study deeper.

## References

- [1] A. Satter, G. M. Iqbal and J. L. Buchwalter, Practical Enhanced Reservoir Engineering: Assisted with Simulation Software., PennWell, 2008.
- [2] Schlumberger, Oilfield Review Autumn 2012., 2012.
- [3] G. Brown, D. Storer, K. McAllister, M. Al-Asimi and K. Raghavan, SPE-84379. Monitoring Horizontal Producers and Injectors During Cleanup and Production Using fiber-Optic distribute Temperature Measurements, Denver: Society of Petroleum Engineers, 2003.
- [4] M. Tolan, M. Boyle and G. Williams, SPE-71676. The Use of Fiber-Optic Distributed Temperature Sensing and Remote Hydraulically Operated Interval Control Valves for the Management of Water Production in the Douglas Field, Society of Petroleum Engineers, 2001.
- [5] H. Foucault, D. Poilleux, A. Djuricic, M. Slikas, J. Strand and R. Silva, SPE-89405A. Successful Experience for Fiber Optic and Water Shut Off on Horizontal Wells With Slotted Liner completion in an Extra Heavy Oil Field, Tulsa: Society of Petroleum Engineers, 2004.
- [6] S. Storås, Master Thesis. Low Salinity EOR-potential for Yme at Reservoir Conditions - An Experimental Study, University of Stavanger, 2012.
- [7] D. Håmsø, Master Thesis. Adsorption of quinoline onto illite at high temperature in relation to low salinity waterflooding in sandstone reservoirs, University of Stavanger, 2011.
- [8] T. Austad, S. Strand, M. V. Madland, T. Puntervold and R. Korsnes, "SPE-118431-PA. Seawater in Chalk: an EOR and Compaction Fluid.," Society of Petroleum Engineers, 2008.
- [9] A. R. Sagi, M. Puerto, Y. Bian, C. A. Miller and G. J. Hirasaki, SPE-164062-MS. Laboratory Studies for Surfactant Flood in Low-Temperature, Low-Salinity Fractured Carbonate Reservoir., Society of Petroleum Engineers, 2013.
- [10] J. J. Taber, F. D. Martin and R. S. Seright, SPE-39234-PA. EOR Screening Criteria Revisited Part 2: Applications and Impact of Oil Prices., Society of Petroleum Engineers, 1997.
- [11] K. Skrettingland, E. Dale, V. Stenerud, A. M. Lambertsen, K. Kulkarni, A. Stavland and Ø. Fevang, SPE-169727-MS. Snorre In-depth Water Diversion Using Sodium Silicate – Large Scale Interwell Field Pilot, Society of Petroleum Engineers, 2014.
- [12] M. Dallard and J. E. Hanssen, SPE-35375. Foam application in North Sea reservoirs, II: efficient Selection of Products for Field Use, Society of Petroleum Engineers, 1996.
- [13] A. R. Awan, R. Teigland and J. Kleppe, SPE-99546-PA. A Survey of North Sea Enhanced-Oil-Recovery Projects Initiated During the Years 1975 to 2005., Society of Petroleum Engineers, 2008.

- [14] Ø. Dugstad, "Chapter 6. Well-to-Well Tracer Tests," in *Reservoir Engineering Handbook Volume 5*, Second Edition ed., Society of Petroleum Engineers, 2007.
- [15] Schlumberger, "Web literature," [Online]. Available: [www.slb.com](http://www.slb.com).
- [16] Schlumberger, Oilfield Review Spring 2012., 2012.
- [17] P. Tipler and G. Mosca, *Physics for Scientists and Engineers, Volume 1 (6th ed.)*, Worth Publishers, 2008.
- [18] L. Guan and Y. Du, SPE 89956-MS. Will Tracer Move the Same Velocity as Its Carrier?, Society of Petroleum Engineers, 2004.
- [19] S. Buckley and M. Leverett, SPE942107-G. Mechanism of Fluid Displacement in Sands, Society of Petroleum Engineers, 1942.
- [20] H. Lauwerier, "The transport of heat in an oil layer caused by the injection of hot fluid," in *Applied Scientific Research, Section A. Vol 5 (19-15)*, p.145, Applied Scientific Research, 1955.
- [21] L. Rubinstein, "Doklady Akademii Nauk SSR, Vol.146, p805," 1962.
- [22] A. Zolotukhin, "SPE-7964. Analytical Definition Of The Overall Heat Transfer Coefficient," Society of Petroleum Engineering, 1979.
- [23] R. J. Platenkamp, SPE13746-MS. Temperature Distribution Around Water Injectors: Effects on Injection Performance, Society of Petroleum Engineers, 1985.
- [24] N. Arihara, A study of nonisothermal single and two-phase flow through consolidated sandstones., Stanford Geothermal Program, 1974.
- [25] Computer Modelling Grp. Ltd., "STARS User Guide," 2014.
- [26] Computer Modelling Grp. Ltd., GEM User Guide., 2014.
- [27] Computer Modelling Grp. Ltd., PAPER 2009-308. Flexible Wellbore Model Coupled to Thermal Reservoir Simulator., World Heavy Oil Congress, 2009.
- [28] C. P. Andrews-Speed, E. R. Oxburgh and B. A. Cooper, "Temperatures and Depth-Dependent Heat Flow in Western North Sea," *AAPG Bulletin*, pp. p. 1764-1781, 1984.